NASA CONTRACTOR REPORT

NASA CR-1421

THE TRANSIENT RESPONSE OF COUPLED ACOUSTO-MECHANICAL SYSTEMS

by A. Craggs

Prepared by
UNIVERSITY OF SOUTHAMPTON
Southampton, England
for Langley Research Center

NATIONAL AERONAUTICS AND SPACE ADMINISTRATION • WASHINGTON, D. C. • AUGUST 1969

NASA CR-1421

THE TRANSIENT RESPONSE OF COUPLED ACOUSTO-MECHANICAL SYSTEMS

By A. Craggs

Prepared under Grant No. NGR 52-025-003 by
UNIVERSITY OF SOUTHAMPTON
Southampton, England

for Langley Research Center

NATIONAL AERONAUTICS AND SPACE ADMINISTRATION

For sale by the Clearinghouse for Federal Scientific and Technical Information
Springfield, Virginia 22151 – CFSTI price $3.00

THE TRANSIENT RESPONSE OF COUPLED ACOUSTO-MECHANICAL SYSTEMS

By A. Craggs

SUMMARY

The behaviour of a coupled plate-acoustic cavity system is studied using a computer orientated technique. The work is divided into two parts. In the first part some simplifying assumptions are made about the nature of the cavity pressure; it is assumed to be uniform and a function of the volume displacement of the boundary. The plate system is represented by an assemblage of rectangular finite elements and the equations of motion are expressed in terms of displacements; the effect of the cavity is simply to introduce an extra stiffness matrix term. In the second part the simplifying assumptions are removed and both the plate and acoustic systems are idealised using finite elements - the acoustic system being formulated in terms of pressures.

The results show that where the window is large and flexible, and the cavity small, the in vacuo normal modes become coupled and there is a change in the natural frequencies of the system, and consequently a considerable modification to the in vacuo response. The acoustic finite element results show that in the frequency range excited by sonic booms the acoustic responses of a room with one flexible window are dominated by the lower plane-wave depth modes. However, near the window the effects of the non-propagating cut-off modes are significant.

SYMBOLS

w	displacement
$\{w\}$	displacement response vector
q_{ij}	generalised coordinates
p	pressure
$\{p\}$	pressure response vector
ϕ	velocity potential
x,y,z	spatial coordinates
i,j,ℓ,m,n	integer mode suffices
a,b	plate element dimensions

d	depth of cavity
ω	frequency
ψ_i	i th plate mode
ω_i	natural frequency of the ith mode
β	aspect ratio for the plate
v_o	cavity volume
η	ratio of acoustic to mechanical stiffness
E	Young's modulus
h	plate thickness
μ	Poisson's ratio
ρ_p	plate density
ρ_a	density of air
c	velocity of sound in air
TE	kinetic energy (expressed in terms of displacements)
VE	strain energy " " " " "
BE	work function
TE*	kinetic energy (expressed in terms of force like quantities)
VE*	strain energy " " " " " " "
BE*	work function
$[M]$	mass matrix
$[K]$	stiffness matrix
$[P]$	acoustic "mass" matrix
$[S]$	acoustic "stiffness" matrix
$[\theta]$	rectangular coupling matrix
$\{F\}$	force vector
$[B_o]$	Boolean transformation matrix. Relates element coordinates to global system coordinates.
f_i, g_i	Hermitian interpolation polynomials

PART 1 APPLICATION OF VOLUME DISPLACEMENT THEORY

INTRODUCTION

This part of the work is concerned with the response of a coupled plate-acoustic system where the acoustic wavelength is large in comparison with the dimensions of the enclosure. The main objectives are: (i) to extend the finite element method to deal with this situation; (ii) to observe the changes brought about in the plate mode shapes and natural frequencies by the presence of the cavity; (iii) to observe the behaviour of the coupled systems when excited by an ideal 'N' wave.

When the acoustic wavelength is large, the excess pressure in the cavity is uniform throughout and is directly proportional to the volume displacement of the boundaries; the cavity then has a stiffening action on the plate. Several studies have already been made with these simplifying assumptions. Lyon (1) used this approach when considering the low frequency noise reduction through a rectangular enclosure with one flexible wall, though the analysis was restricted to the case where the panel modes and frequencies were little affected by the enclosure. Pretlove (2) when studying the effects of a backing cavity on a plate with large aspect ratio assumed the pressure was uniform and proportional to the volume displacement obtained an exact solution to the problem. Dowell and Voss (4) and (5) and later Pretlove (3) drew similar conclusions about the effect of a shallow cavity on a flexible panel after using a series solution for the acoustic velocity potential. In the above references the work was concerned with a simple plate panel; the volume displacement approach has been used on a more general configuration by Lyon et al (6) when dealing with the low frequency noise reduction of space-craft structures.

The work is divided into four main sections: the first section is concerned with obtaining limits for the application of volume displacement theory by studying a one-dimensional acousto-mechanical model; the second section extends the finite element plate theory to include the effect of the cavity; this is achieved by the formation of an additional stiffness matrix which couples all of the available degrees of freedom. The procedure is applicable to a structure of any shape which may be idealised by an assembly of finite elements. However, this work is restricted to structures which may be built up from rectangular elements. The final sections are concerned with the numerical solution of the equations of motion, for the eigenvalue problem and the step by step solution for the forced transient response respectively and some consideration is given to the effect of a leakage in the cavity on the motion of the plate.

DISCUSSION ON THE EXACT SOLUTION FOR A SIMPLE SYSTEM

In this section the free vibration of a simple plate-acoustic cavity system is discussed in order to illustrate its salient features. The type of system under consideration is shown in Figure 1.

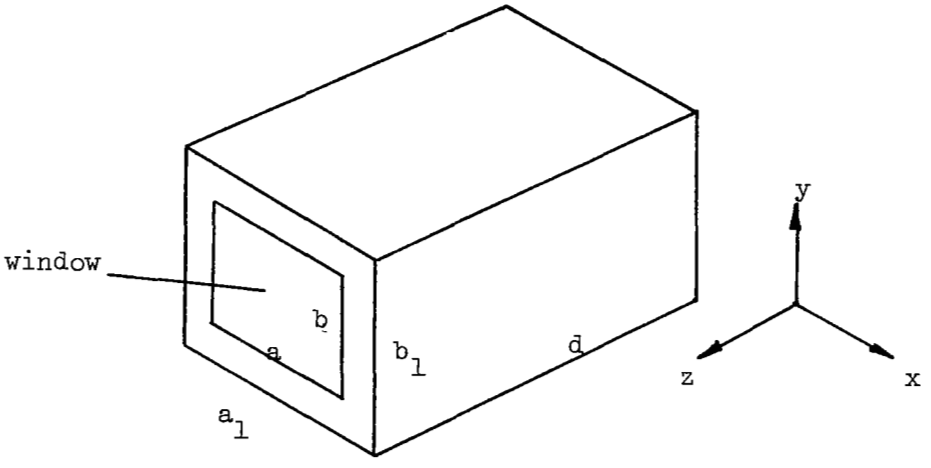

Figure 1. Simple Plate-Cavity System.

The differential equation governing the motion of the plate is:

$$\ddot{w} + \frac{Eh^2}{12\rho(1-\mu^2)} \nabla^4 w = -\frac{p}{\rho h} ; \qquad (1)$$

and the equation governing the acoustic back pressure is

$$\frac{1}{c^2}\ddot{p} - \nabla^2 p = 0 \qquad (2)$$

The two systems are linked by the dynamic boundary condition at the acoustic plate interface:

$$\frac{\partial p}{\partial z} = \rho\ddot{w} \qquad (3)$$

If the plate is simply supported the motion of the plate may be expressed in terms of an infinite series of double sine modes:- $q_{ij} \sin\frac{i\pi x}{a} \sin\frac{j\pi y}{b}$. Equation (1) then becomes:

$$\sum_i^\infty \sum_j^\infty q_{ij} \sin\frac{i\pi x}{a} \sin\frac{j\pi y}{b} + \frac{Eh2}{12\rho(1-\mu^2)} \sum_i^\infty \sum_j^\infty \nabla^4 q_{ij} \sin\frac{i\pi x}{a} \sin\frac{j\pi y}{b} = -\frac{p_b}{\rho h} \qquad (4)$$

Providing there are no internal acoustic sources, the acoustic back pressure is induced solely by the plate motion and its effect is to couple the in-vacuo principal modes of the plate. If the cavity in Fig. 1 has hard walls and the motion of the coupled system proceeds with a time dependence of the form $\sin \omega t$, then the back pressure may be shown to have the form (ref. 3)

$$p_b = \{A_o \cos \frac{\omega z}{c} + \sum\sum_{\infty\infty} A_{mn} \cos \frac{m\pi x}{a_1} \cos \frac{n\pi y}{b_1} \cosh \Omega_{mn} z\} \sin \omega t \qquad (5)$$

where $m + n > 0$

$$\Omega_{mn}^2 = \frac{\omega^2}{c^2} - \pi^2 \left(\frac{m^2}{a_1^2} + \frac{n^2}{b_1^2}\right)$$

The magnitude of the coefficients A_o and A_{mn} are dependent upon the dynamic boundary conditions at the plate-cavity interface. The term A_o represents the pressure due to plane wave modes which propagate perpendicular to the rear face of the window along the depth of the cavity. The terms multiplied by A_{mn} correspond to the 'cross modes'. It may be noted that the term Ω_{mn} may be entirely real or entirely imaginary, depending on the frequency, ω, and the mode integers m and n. If Ω is real, then the mode does not propagate; most of the pressure fluctuations occurring locally at the rear face of the window. If Ω is imaginary then the mode propagates along the cavity.

Simplified Frequency Equations

An exact solution to equations (4) and (5) has been given by Pretlove (3) for the case where the window completely covers one wall. In what follows some low frequency restrictions are imposed: the plate is represented by its first three in-vacuo volume displacing normal modes; in treating the acoustics, only plane waves are considered, so that the effects of the cross modes are neglected. This latter assumption is reasonable as the cross modes do not propagate at frequencies below their cut-off frequency.

The plate equation becomes, in terms of the three generalised co-ordinates:

$$\ddot{q}_{ij} + \omega_{ij}^2 q_{ij} = -\frac{p_b}{\rho_p h} \frac{16}{ij\pi^2}; \qquad i,j = 1,1;\ 3,1;\ 1,3. \qquad (6)$$

The acoustic equation simply becomes

$$p_b = A \cos \frac{\omega z}{c} \qquad (7)$$

Now, the essential boundary conditions at the interface are given by equation (3) but, because of the effective constraints that have been applied to both systems, the condition cannot be satisfied at every point of the surface. Instead, the equilibrium of the whole surface is satisfied thus:

$$\int_0^b \int_0^a \rho \ddot{w}(x, y)\,dxdy = \int_0^{b_1} \int_0^{a_1} \left(\frac{\partial p}{\partial z}\right)_{z=\ell} dxdy$$

Hence, on substituting for w and p,

$$-\rho\omega^2 \sum q_{ij} \int_0^b \int_0^a \sin \frac{i\pi x}{a} \sin \frac{j\pi y}{b}\,dxdy = \frac{A\omega}{c} \sin \frac{\omega \ell}{c} \int_0^b \int_0^a dxdy$$

This latter equation gives an expression for A, which in turn may be substituted into eq. (7) for the acoustic back pressure. Then substituting for p_b in eq. (6) gives

$$\ddot{q}_{ij} + \omega_{ij}^2 q_{ij} = -\frac{64}{ij\pi^4} \frac{\rho_a c \omega}{\rho_p h} \frac{ab}{a_1 b_1} \cot \frac{\omega d}{c} \sum \frac{q_{ij}}{ij} \qquad (8)$$

If a state of free vibration exists so that $\ddot{q}_{ij} = -\omega^2 q_{ij}$, then the frequency equation for the system is:-

$$\begin{vmatrix} \omega_{11}^2 + c_1 - \omega^2 & c_1/3 & c_1/3 \\ c_1/3 & \omega_{13}^2 + \frac{c_1}{9} - \omega^2 & c_1/9 \\ c_1/3 & c_1/9 & \omega_{31}^2 + \frac{c_1}{9} - \omega^2 \end{vmatrix} = 0 \qquad (9)$$

$$c_1 = \frac{64}{\pi^4} \frac{\rho_a c}{\rho_p h} \frac{ab}{a_1 b_1} \cot \frac{\omega d}{c}$$

Now, as stated previously, this equation allows for the roots due to

acoustic standing waves. The volume displacing theory applies when the acoustic pressure is nearly uniform throughout the enclosure. In which case $(\omega\ell/c)$ is small and $\cos(\omega\ell/c) \doteq 1$; $\sin(\omega\ell/c) \doteq \omega\ell/c$; so that $\cot(\omega\ell/c) \doteq c/\omega\ell$. However, it is informative to adopt the approach which is to be used in the ensuing sections to derive the "volume-displacement" frequency equation.

If the process is adiabatic, the back pressure is a function of the volume displacement of the boundaries and is given by:

$$p_b = \frac{\rho_a c^2}{v_o} \delta v$$

where v_o is the volume of the enclosure = $a_1 b_1 d$.

Now
$$\delta v = \int_0^b \int_0^a q_{ij} \sin \frac{i\pi x}{a} \sin \frac{j\pi y}{b} \, dxdy, \qquad i,j = 1,1;\ 3,1;\ 1,3.$$

Therefore
$$p_b = \frac{4\rho c^2}{\pi^2 \ell} \frac{ab}{a_1 b_1} \sum \frac{q_{ij}}{ij}$$

Then, after substituting for p_b in eq. (6), the frequency equation becomes:

$$\begin{vmatrix} \omega_{11}^2 + c_2 - \omega^2 & c_2/3 & c_2/3 \\ c_2/3 & \omega_{13}^2 + c_2/9 - \omega^2 & c_2/9 \\ c_2/3 & c_2/9 & \omega_{31}^2 + c_2/9 - \omega^2 \end{vmatrix} = 0 \qquad (10)$$

where $c_2 = \frac{64}{\pi^4} \frac{\rho_a c^2}{\rho_p h d} \frac{ab}{a_1 b_1}$.

Results.- The roots of the two frequency equations (9) and (10) were evaluated for a glass plate of dimensions 144" x 96" x 0.25", with a backing cavity of air of dimensions 144" x 96" x d". The depth of the cavity, d, was varied from 120" to 900". It was also of interest to compare the roots obtained from the diagonal terms of eq. (10), only; these imply that there is no change in the mode shape and no coupling

between the modes.

The results shown in Fig. 2 illustrate two points. The first, and most important, is that the volume displacing theory gives results which are well within 5% of the exact plane wave solutions for the short cavity depths, i.e. $1/d'' > .05$. The accuracy decreases as the plate modes begin to excite a standing wave down the depth of the enclosure, the frequency of the standing wave being that given by $\omega_c = c/4d$. When the plate in-vacuo frequencies are greater than ω_c then the enclosure acts as an added mass and the volume displacement theory does not apply. From the results it seems that this restriction need only be applied to the first mode as this is affected most and a reasonable criterion for the theory to apply is that the fundamental frequency of the mechanical system should be less than $\omega_c/2.0$.

The natural frequencies obtained by assuming that the modes are uncoupled are very unsatisfactory for small cavity depths and thus the assumption is incorrect. For larger volumes the frequencies approach the volume displacement values, but neither theory is then correct as the cavity is then inertia controlled.

Definition of η, the ratio of acoustic to mechanical stiffness.- This definition is derived from the acoustic and mechanical stiffnesses of the fundamental mode for a simply supported plate enclosing a volume v_o of compressible fluid.

The mechanical stiffness is $\dfrac{\pi^4 Eh^3}{12(1-\mu^2)a^4} \quad \dfrac{(1+\beta^2)^2}{\beta^4}$

The acoustic stiffness is $\dfrac{64\rho c^2}{\pi^4 v_o} \beta a^2$

$$\eta = \frac{768(1-\mu^2)}{\pi^8} \frac{\rho c^2}{E} \quad \frac{\beta^5}{(1+\beta^2)^2} \quad \frac{a^6}{v_o t^3} \qquad (11)$$

This definition is to hold for other boundary conditions although it is not the true value. Typical values of η for an average room are given in the table below for a plate aspect ratio $\beta = b/a = 2.0$; $v_o = 2.0 \times 10^6$ cubic ins.

	Window dimensions			
	40 x 20 x 0.125	80 x 40 x .1875	120 x 60 x .25	168 x 84 x .25
η	3.28×10^{-3}	6.19×10^{-2}	3.2×10^{-1}	2.5

PLATE FINITE ELEMENT FORMULATION TO INCLUDE CAVITY STIFFNESS EFFECTS

In this report only rectangular finite elements are considered. The method consists of dividing the plate into a number of these elements, and within each element the displacement is given by a number of assumed modes, the coefficients of each mode being related to the modal displacements. Here four displacement unknowns per element corner are used; these are w, $\partial w/\partial x$, $\partial w/\partial y$, $\partial^2 w/\partial x \partial y$. The assumed modes are Hermitian interpolation polynomials having the properties:

	f	$f'(o)$	$f(1)$	$f'(1)$
$f_1(\xi) = 1 - \xi^2 + 2\xi^3$	1	0	0	0
$f_2(\xi) = \xi - 2\xi^2 + \xi^3$	0	1	0	0
$f_3(\xi) = 3\xi^2 - 2\xi^3$	0	0	1	0
$f_4(\xi) = \xi^3 - \xi^2$	0	0	0	1

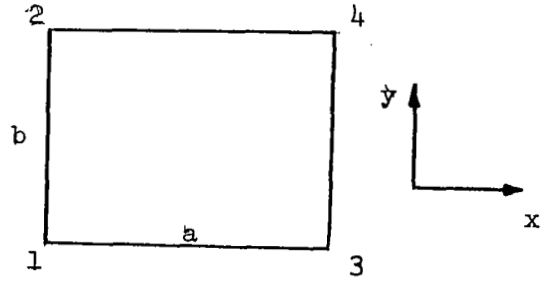

$$X = \frac{x}{a}$$

$$Y = \frac{y}{b}$$

For the above plate element

$$\begin{aligned} w(x,y) = {} & w_1 f_1(X) f_1(Y) + a\left(\frac{\partial w}{\partial x}\right)_1 f_2(X) f_1(Y) + b\left(\frac{\partial w}{\partial y}\right)_1 f_1(X) f_2(Y) + ab\left(\frac{\partial^2 w}{\partial x \partial y}\right)_1 f_2(X) f_2(Y) \\ & + w_2 f_1(X) f_3(Y) + a\left(\frac{\partial w}{\partial x}\right)_2 f_2(X) f_3(Y) + b\left(\frac{\partial w}{\partial y}\right)_2 f_1(X) f_4(Y) + ab\left(\frac{\partial^2 w}{\partial x \partial y}\right)_2 f_2(X) f_4(Y) \\ & + w_3 f_3(X) f_1(Y) + a\left(\frac{\partial w}{\partial x}\right)_3 f_4(X) f_1(Y) + b\left(\frac{\partial w}{\partial y}\right)_3 f_3(X) f_2(Y) + ab\left(\frac{\partial^2 w}{\partial x \partial y}\right)_3 f_4(X) f_2(Y) \\ & + w_4 f_3(X) f_3(Y) + a\left(\frac{\partial w}{\partial x}\right)_4 f_4(X) f_3(Y) + b\left(\frac{\partial w}{\partial y}\right)_4 f_3(X) f_4(Y) + ab\left(\frac{\partial^2 w}{\partial x \partial y}\right)_4 f_4(X) f_4(Y) \end{aligned}$$

$$w(x, y) = \{w_e\}^T\{f_X f_Y\} = \{f_X f_Y\}^T\{w_e\} \qquad (12)$$

The equations of motion are deduced from Hamilton's principle, which states that between two instants of time t_1 and t_2 the motion proceeds in such a way that the "action" integral

$$J = \int_{t_1}^{t_2} (TE - (VE_m + VE_c) + BE)dt$$

is stationary for the actual motion when compared with all other possible motions taking on the prescribed actual values at t_1 and t_2. VE_m is the mechanical strain energy, VE_c is the acoustic strain energy of the cavity. When the energies are expressed in terms of displacements the principle leads to the Euler Lagrange equation

$$\frac{\partial}{\partial t}\left(\frac{\partial TE}{\partial \dot{q}_i}\right) + \frac{\partial VE_m}{\partial q_i} + \frac{\partial VE_c}{\partial q_i} = \frac{\partial BE}{\partial q_i} \qquad (13)$$

Now, the element mass and stiffness matrices for the purely mechanical terms have already been given by Mason (7). The mass matrix is:

$$[M_e] = \rho h \int_0^b \int_0^a \{f_X f_Y\}\{f_X f_Y\}^T \, dxdy$$

The stiffness matrix is

$$[K_e] = \frac{Eh^3}{12(1-\mu^2)} \int_0^b \int_0^a (\{f_X'' f_Y\}\{f_X'' f_Y\}^T + \{f_X f_Y''\}\{f_X f_Y''\}^T + \mu\{f_X'' f_Y\}\{f_X f_Y''\}^T$$
$$\ldots \mu\{f_X f_Y''\}\{f_X'' f_Y\}^T + 2(1-\mu)\{f_X'' f_Y''\}\{f_X'' f_Y''\}^T \, dxdy$$

where the dashes denote spatial derivatives.

The forcing vector for a pressure $P(x,y,t)$ on the element surface

$$\{F_e\} = \gamma \int\int \{f_X f_Y\} P(x,y,t)dxdy$$

where $\gamma = \text{diag}\{1, a, b, ab, 1, a, b, ab, 1, a, b, ab, 1, a, b, ab\}$.

The equations of motion for each element are:

$$[M_{e_1}]\{w_e\}_1 + [K_{e_1}]\{w_e\}_1 = \{F_e\}_1$$

$$[M_{e_2}]\{w_e\}_2 + [K_{e_2}]\{w_e\}_2 = \{F_e\}_2$$

$$\cdot \quad \cdot \quad \cdot \quad \cdot \quad \cdot$$

$$[M_{e_n}]\{w_e\}_n + [K_{e_n}]\{w_e\}_n = \{F_e\}_n$$

and these can be written as a single matrix equation

$$[M_u]\{w_u\} + [K_u]\{w_u\} = \{F_u\}. \qquad (14)$$

At this stage the elements are still not linked together. The systems are assembled by considering equilibrium and compatibility conditions. If $\{w\}$ is the displacement vector for the overall system and $\{F\}$ is the force vector, then these are related to $\{w_u\}$ and $\{F_u\}$ by means of a rectangular Boolean matrix $[B_o]$ which contains only ones and zeroes

$$\text{for compatibility} \qquad \{w_u\} = [B_o]\{w\} \ ;$$

$$\text{for equilibrium} \qquad \{F\} = [B_o]^T\{F_u\} \ ;$$

substituting for $\{w_u\}$ and $\{F_u\}$ in eq. (14) gives the equation of motion for the assembled system:

$$[B_o]^T[M_u][B_o]\{\ddot{w}\} + [B_o]^T[K_u][B_o]\{w\} = \{F\} \qquad (15)$$

Because no constraints have been applied and the assembled system is free to move in space, the matrix $[B_o]^T[K_u][B_o]$ is singular. Constraints are applied by making the displacement zero at a particular point and necessitates removing appropriate rows and columns from the mass and stiffness matrices. If N constraints are applied then the order of the matrices is reduced by N.

The Acoustic Stiffness Matrix

In the above the effect of the cavity has been neglected. Its effect will now be given by considering the variation of the cavity strain energy term, VE_c.

$$VE_c = \tfrac{1}{2} \frac{\rho c^2}{V_o} \delta v^2 \tag{16}$$

The volume displacement for an element is

$$\delta v_t = \underset{\sim}{w}_t^T \int_S \{f_X f_Y\} dS = \underset{\sim}{w}_e^T \underset{\sim}{G}_i$$

The total volume displacement for an assembly of N finite elements

$$\delta v_T = \sum_i^N \{w_i\}^T \int_S \{f_X f_Y\}$$

and this can be expressed in the more convenient matrix form

$$\delta v_T = \underset{\sim}{w}_o^T \hat{\underset{\sim}{G}}$$

where $\underset{\sim}{w}_o$ and $\hat{\underset{\sim}{G}}$ are column vectors defined by

$$\underset{\sim}{w}_o = \begin{bmatrix} \underset{\sim}{w}_1 \\ \underset{\sim}{w}_2 \\ \underset{\sim}{w}_3 \\ \vdots \\ \underset{\sim}{w}_N \end{bmatrix} \qquad \hat{\underset{\sim}{G}} = \begin{bmatrix} \underset{\sim}{G}_1 \\ \underset{\sim}{G}_2 \\ \underset{\sim}{G}_3 \\ \vdots \\ \underset{\sim}{G}_N \end{bmatrix}$$

where the integer suffices refer to the element number.

The total VE_c for the assemblage of elements is then:

$$VE_c = \tfrac{1}{2} \frac{\rho c^2}{V_o} \underset{\sim}{w}_o^T \hat{\underset{\sim}{G}} . \hat{\underset{\sim}{G}}^T \underset{\sim}{w}_o \tag{17}$$

At this stage the elements are unassembled. The assembly is carried out by relating the element coordinates to the assembled system coordinates using the Boolean transform matrix.

$$\{w_o\} = [B_o]\{w\}$$

Then in terms of the system coordinates

$$U_c = \tfrac{1}{2}\{w\}^T \frac{\rho c^2}{v_o} [B_o]^T \{\hat{G}\}\{\hat{G}\}^T [B_o]\{w\}^T$$

and this gives the additional unconstrained stiffness matrix due to the cavity as:

$$[K_{cavity}] = \frac{\rho c^2}{v_o} [B_o]^T \{\hat{G}\}\{\hat{G}\}^T [B_o] \qquad (18)$$

Plate linked through the Cavity to a Set of Leaks

The leak terms are treated as simple Helmholtz resonators where the leak mass oscillates on the spring provided by the cavity. In this case the cavity strain energy is

$$VE_c = \tfrac{1}{2} \frac{\rho c^2}{v_o} (\delta v_p^2 + 2\delta v_p \delta v_L + \delta v_L^2)$$

where δv_p and δv_L are the volume displacements of the leaks and plate respectively.

For a number of leaks of area a_i and displacements d_i then

$$\delta v_L = \sum a_i d_i = \{a_i\}^T \{d_i\}.$$

The variation of VE_c with respect to all the coordinates gives rise to three different stiffness matrices: the first corresponding to the plate volume displacement is that given by equation (18) in the previous section. A second direct stiffness matrix obtained by the variation of the v_L^2 term for the leaks is:

$$[K_{LL}] = \frac{\rho c^2}{v_o} \{a_i\}\{a_i\}^T \qquad (19)$$

The plate and leaks are linked by the coupling matrix derived by the variation of the $v_p v_L$ term. This is given by

$$[K_{pL}] = \frac{\rho c^2}{v_o} [B_o]^T \{\hat{G}\}\{a_i\}^T \qquad (20)$$

The stiffness matrix for the whole system is then of the form

$$\left[\begin{array}{c|c} K_{pp} & K_{pL} \\ \hline K_{pL}^{T} & K_{LL} \end{array}\right] \qquad (21)$$

The leakage terms also contribute to the kinetic energy, so that additional terms are needed in the mass matrix when dealing with the complete system. These are all simple diagonal terms given by:

$$\rho a_i \ell_i$$

where ℓ_i is the equivalent length of the i^{th} leak.

The Nature of the Cavity Stiffness Matrix

The essential feature of the cavity stiffness matrix may be deduced from equation (17). This shows that it can only be constructed by dealing with the system as a whole. All degrees of freedom are linked by the cavity matrix; unlike the mechanical stiffness matrix which is usually fairly sparsely populated, such that there is no cross linkage between many of the degrees of freedom.

If the plate is idealised using elements of equal dimensions the cavity stiffness before being assembled has the form:

$$\begin{bmatrix} \alpha & \alpha & \cdots & \alpha \\ \alpha & \alpha & & \alpha \\ \alpha & \vdots & \ddots & \\ \vdots & \vdots & & \alpha \\ \alpha & \alpha & \alpha & \alpha \end{bmatrix}$$

where α is a square symmetric matrix given by:

$$\alpha = \frac{\rho c^2}{v_o} \int_0^b \int_0^a \{f_X f_Y\}\, dxdy \int_o^b \int_o^a \{f_X f_Y\}^T dxdy$$

where a and b are element dimensions.

Because α is a column vector multiplied by its transpose, both α and the cavity stiffness matrix are singular, and of rank 1. This feature is not unexpected though because a disturbance at one point produces a uniform pressure over the whole surface of the plate.

THE EIGENVALUE PROBLEM

Using the notation of the previous section the equation of motion of a plate-cavity configuration may be put in the form

$$[K_m + K_{cav} - \omega^2 M]\{w\} = 0 \qquad (22)$$

The effects of altering the cavity volume and hence η is achieved simply by multiplying K_{cav} by an appropriate scaling factor. Various plate boundary conditions may be applied simply by removing the appropriate rows and columns of the assembled matrices.

A FORTRAN program was written to solve equation (22) for various configurations. The purpose of the investigation was to examine the effect of varying η, on a rectangular plate with all edges simply supported, and a plate with all edges clamped. The effect of aspect ratio was also considered. Throughout the work plate finite elements with four unknowns per corner, that is, w, $\partial w/\partial x$, $\partial w/\partial y$ and $\partial^2 w/\partial x \partial y$, as these had been shown previously, Mason (7), to give the most satisfactory solution for plates in in-vacuo conditions.

A preliminary study was first made in order to check the formation of K_{cav}; since only the volume displacing modes of the plate cause any change in strain energy, UE_c, then these would be the only modes to increase in frequency when the volume of the cavity is reduced. In Fig. 3 this is shown to be the case; the non volume displacing modes are unaffected.

The results of Fig. 3 were obtained by using four plate elements, and as mentioned above, the idealisation included the asymmetric non volume displacing modes. Subsequent results were found by using properties of symmetry, such that the 4 element idealisation was equivalent to an idealisation with 16 elements, the contributions from the asymmetric modes being removed, so that all eigenvalues and vectors which were evaluated referred to the volume displacing modes and these are the only ones referred to in the following discussion.

Results

Figs. 4 and 5 are results for a clamped and simply supported plate. These show that in the range of η studied the lowest modes are the most affected. In both cases the fundamental mode first increases rapidly with increase in η and then the frequency appears to approach a constant value nearly equal to the in vacuo natural frequency of the second volume displacing mode. While the rate of change of natural frequency of the first mode is slowing down, the change of frequency of the second mode increases. An explanation of this phenomenon is given by referring to the new normal modes of the system.

The normal modes for the first and second frequencies are shown in Fig. 6 and Fig. 7. These modes have been normalised by dividing by the deflection at the plate centre. In the range of η considered in the computations these modes are various combinations of the first two in vacuo modes, and at small values of η, when the natural frequencies have only increased slightly, the mode shapes are virtually unchanged. However, as η increases the coupling between modes becomes evident and the modes lose their characteristic shape. The reason for the behaviour of the natural frequencies then becomes evident: the first mode stops increasing in frequency because the two in vacuo volume displacing modes combine to form a near non-volume displacing mode. For the simply supported case the in vacuo coefficients q_{11} and q_{13} are such that:

$$\int\int q_{13} \sin \frac{\pi x}{a} \sin \frac{\pi y}{b} \, dxdy + \int\int q_{13} \sin \frac{\pi x}{a} \sin^3 \frac{\pi y}{b} \, dxdy = 0$$

i.e. $q_{13} = -3q_{11}$.

For the second mode there is an increased volume displacement and hence the increased rate of change of frequency. Although the point is not illustrated it would seem that a similar occurrence would also occur at the higher modes; although in stating this the restrictions of the theory, i.e. that a state of uniform pressure exists throughout the volume, should be remembered.

Now it has already been mentioned that as η increases the frequency of the first mode increases until it is near the natural frequency of the second mode. It then appears to approach this frequency asymptotically. With this in mind then, it is obvious that the behaviour is dependent upon the frequency ratio of the first two in vacuo modes. This ratio is a function of the aspect ratio, β, and for a simply supported plate it is given by:

$$\left(\frac{\lambda_{13}}{\lambda_{11}}\right)^2 = \left(\frac{\beta^2 + 9}{\beta^2 + 1}\right)^2.$$

The equation shows that the frequency ratio decreases as the aspect ratio is increased, and hence the asymptotic effect will occur for small values of η with increasing aspect ratio. Figs. 8 and 9 show the computed results for $(\lambda/\lambda_{vacuo})^2 \sim \eta$, for different aspect ratios and for different plate boundary conditions. The in vacuo frequency ratios computed for the first two modes are also shown where they fit on the curves. The results are in general agreement with those suggested in this discussion. The clamped plate does not respond to the same degree because η is not the true value for the acoustic to mechanical stiffness ratio.

The behaviour of the first two modes is important as it is these modes which will dominate the stress distribution. That which is of particular importance, when η is large, is when the two volume displacing modes combine to form a near non-volume displacing mode; this mode, ψ, will not be excited under a uniform pressure load, p, because the generalised force is nearly zero, i.e.

$$p \int_S \psi dS \doteq 0.$$

This means that the stress distribution will then be covered by the second mode, which Figures 6 and 7 show that, in the longitudinal direction, the maximum curvature and hence the maximum bending stress moves towards the edges.

The results for a square clamped plate are shown in Fig. 10; this configuration does not fit into the general pattern of behaviour. The theory which applies for the other aspect ratios indicates that two volume displacing modes occur with equal natural frequencies. According to Warburton (8), this does not occur; instead, there are two 'degenerate' modes with slightly different frequencies. The lowest of these degenerate modes has nodal lines across the diagonals and is a non-volume displacing mode which, with varying cavity volume, has a constant natural frequency. However, this mode is symmetrical about the quarter plate lines which is the reason its eigenvalue and vector were evaluated in the computed program. The second degenerate mode has a nodal circle about the centre of the plate; this is a volume displacing mode and the diameter of the nodal circle decreases with increase in η.

THE TRANSIENT FORCED VIBRATION OF A COUPLED PLATE-CAVITY SYSTEM

This section is concerned with the transient response of two different plate cavity configurations: the first system is simply a plate covering an airtight enclosure where the loading is applied on the outside surface of the plate. In the second system a leakage

term is allowed which affects the back pressure acting on the inside surface of the plate. This extra term may enhance or diminish the motion of the sealed system. It also changes the frequency characteristic.

The equation of motion for the first system is:

$$[M]\{\ddot{w}\} + [K_m + K_{cav}]\{w\} = \{F_p\} \qquad (23)$$

The equation of motion for the second system allowing for a single leak, is:

$$\begin{bmatrix} M & 0 \\ 0 & \rho a_L \ell_e \end{bmatrix} \begin{Bmatrix} \ddot{w} \\ q_i \end{Bmatrix} \begin{bmatrix} K_m + K_{cav} & K_{p\ell} \\ K_{p_\ell}^T & (\rho c^2/v_o)a_i^2 \end{bmatrix} \begin{Bmatrix} w \\ q_i \end{Bmatrix} = \begin{Bmatrix} F_p \\ F_L \end{Bmatrix} \qquad (24)$$

In this study the effective length ℓ_e was given by $\ell_e = \sqrt{a_L}$.† The time history of the loading parameters F_p and F_L was of the form:

$$p(t) = (1 - 2t/\tau) \qquad t < \tau$$
$$p(t) = 0 \qquad t > \tau.$$

Strictly speaking because the leak is separated from the region of the plate by some distance, Δ, in the direction of propagation of the shock wave, there would be a need to account for a delay term, Δ/c. However, it is implicit in the theory that this delay term is small compared with the fundamental period of the coupled system, because a state of uniform pressure is assumed to exist in the cavity. This being the case then the delay term may be neglected and the two loading functions may be assumed to act simultaneously. The leak then has two main effects on the system. Firstly, it adds an extra degree of freedom and consequently it changes the natural frequencies; the degree of the change depends upon leak area. Secondly, because the leak itself is forced there is an extra back pressure within the cavity; there is a subsequent variation in the time history of the net plate load which changes the form of the response.

The transmitted pressure is given by

$$p_T = \frac{\rho c^2}{v_o} \delta v_t.$$

Thus for a sealed cavity

$$p_T = \frac{\rho c^2}{v_o} \hat{G}^T w(t),$$

†Morse (17) p.234 suggests $0.8\sqrt{a_L}$ for an open tube.

and for an allowance for the leakage displacement $q(t)$

$$p_T = \frac{\rho c^2}{v_o} (\underset{\sim}{F}\, \underset{\sim}{w}(t) + a_L\, \underset{\sim}{q}(t)),$$

where $\underset{\sim}{w}(t)$ and $\underset{\sim}{q}(t)$ have been obtained from the solutions of equations (23) and (24). For the simply-supported plate a much simpler expression can be used, based on the assumption that the fundamental in vacuo mode predominates the plate deflection; the pressure may then be written in terms of the centre plate deflection $q_p(t)$:

$$p_T = \frac{\rho c^2}{v_o} \{\frac{4}{\pi^2} ab\, q_p(t) + a_L q(t)\}.$$

Results

FORTRAN programmes were written for the solution of both equations (23) and (24). This solution was obtained by the standard fourth order Runge-Kutta procedure, the details of which are given in Craggs (9). Usually the step size was chosen to satisfy the criterion for accuracy ($\lambda h = 1.0$) and although there was a slight modification to the maximum value when the step size was halved, the variation was insignificant compared with the changes produced in the response when the system variables were altered, so the larger step size was adhered to throughout the computations.

To avoid overflow it was necessary to multiply the stiffness matrices by a factor of 10^{-6}. The results were amended accordingly after computation. Generally, the calculations refer to a glass plate window of dimensions 144" x 84" x 0.25" and where the volume was not decreased to change η, it was assumed to be 3.0×10^6 ins^3.

In the first set of results the effect of the acoustic-mechanical stiffness ratio η, on the response of a window to an 'N' wave was considered. For these computations no leakage terms were allowed for and the cavity was sealed. When an allowance for a leakage was made the effects of varying the leak area and the relative magnitude of the overpressure on the plate and opening were computed. The internal cavity pressure for these cases are also shown.

Effects of η.- Figs. 11 and 12 show the effect of η on the displacement and velocity responses of a simply supported plate to an 'N' wave of constant duration. When η is increased several changes occur in the response: firstly, the magnitude decreases; secondly, the frequency increases, so that there is a noticeable change in the time history. These changes are nothing more than would be expected with an increase in the

system's stiffness. However, there are secondary effects introduced due to the change in period ratio of the loading and in one case the response during the free vibration is extremely small although there is a significant response during the forced motion. This type of loading effect was discussed in Craggs, ref. 18.

A further change in the response characteristics is brought about by the cavity causing the plate natural frequencies to come closer together and consequently, as η increases, the contribution of the second mode should be more significant. This is clearly illustrated in the velocity responses, figure (12) - velocity being more sensitive to the higher modes than displacement. However, it should be noted that the increased significances of this mode is due almost entirely to the reduction in amplitude of the first mode which is affected more by the cavity stiffness. The effects of reducing the cavity volume on the velocity and displacement shock spectra are shown in Fig. 13. As η is increased, the maxima are reduced though the velocity is affected less than the displacement; because the natural frequencies are increased the peaks, corresponding to an isochronous condition, occur at shorter durations.

Leakage effects.- Fig. 14 compares the displacement responses from the centre of a plate obtained during the forced motion under in vacuo conditions, with a sealed cavity and with a cavity leak coupling. Two interesting effects are illustrated: when the leak is included the plate frequencies are always greater and they increase with the area of the opening; also, the plate displacement in the inward direction decreases and is less than the displacement of the sealed system. However this situation is reversed in the outward direction.

These facts may be explained as follows: with the introduction of the opening there are no pure plate modes, each of the modes involves the participation of the leak to some extent. For most of the cases shown the lowest mode of the system involves predominately leak motion and the displacement of the leak mass and plate are in phase; the second mode is affected more by the plate with the plate and leak in anti-phase to each other. (In both these modes the shape of the plate deflection is approximately that of the lowest in vacuo plate mode.) In Fig. 14, the displacements involve mainly the second mode; the frequency is increased because the two systems are moving in anti-phase, effectively reducing the volume of the cavity relative to each other and consequently increasing the stiffness. The amplitude effect is due to the slower frequency of the leak; such that during the first oscillation of the plate the leak is still creating a decrease in volume, thus increasing the cavity pressure. This increased pressure resists the inward movement of the plate and assists the movement outwards.

The above statements refer specifically to the early phases of the

response. The remaining vibration is influenced more by the lowest mode of the system particularly for the larger openings, where this mode subsequently dominates the response. These effects are shown in Fig. 15. However, in order to explain the results it is expedient first to examine the manner in which the natural frequencies and system mode shapes vary with the area of the opening. These are shown in Fig. 16.

The natural frequencies for the volume displacing modes all increase with an increase in the area of the opening, the second natural frequency tending to move away from the first. A simplified version of the system modes is given in the tables alongside the diagram. This simply relates the plate centre displacement relative to that of the leak for the first two modes. An increased value of the ratio, while its modulus is less than unity, is indicative of the amount of coupling between the two sub-systems. There is a strong coupling when the area of the opening is large. This coupling is extremely important; it means that one sub-system cannot move without having a significant effect on the other. The consequence of this will now be discussed in relation to Fig. 15.

The curves for the small openings - 100 and 400 sq. inches – show that the motion is predominantly in the second mode, the first mode effect being indicated by the low frequency beating. In this situation the coupling is weak and the two sub-systems almost vibrate independently at their own natural frequency.

With the larger opening the motion of the plate is more complex and the fundamental mode is dominant, particularly for the 2,500 sq. inch area. This is due to the strong coupling between the two sub-systems which means that the plate is significantly active in the fundamental overall system mode. It is also due to the separation of the two natural frequencies through an increase in the relative stiffness of the second mode which also reduces the second mode's contribution to the response.

Overpressure effects.- The dotted line in Fig. 14 represents the case where the overpressure on the opening is one half that on the plate. The complete set of curves are then representative of two situations for a window over a box-like cavity: one, where the opening is on the same wall as the window and pressure doubling occurs on both sub-systems; the second is where the opening is on the opposite face and pressure doubling occurs only on the window. This, of course, is assuming that the loading is at normal incidence to the window face.

For the small openings there is a significant reduction in the overall response, but the greatest change occurs with the large openings. Again, this is due to the near equal participation of the two sub-systems in the lowest modes. Thus, although a reduction in pressure occurs only at the opening, there is a subsequent reduction in the plate displacement. What is more important in the 2500 sq. inch opening case, and the cause of

the phase lag, is that because of the near-equal participation of the two systems in the second mode, the plate's contribution is reduced by the decrease in overpressure at the opening and hence the rate at which the plate responds is dominated by the frequency of the first system mode.

Internal pressure.- The behaviour of the internal pressure/(maximum free field pressure) ratio, for the various openings and load conditions is shown in Figs. 17 (a) and (b). Three important points are illustrated. The internal pressure is greater than the free field pressure in all cases; this is due to the doubling effects on the surface of the plate, and the dynamic amplification caused by the inertia forces of the plate and leakage mass. The second point is that the pressure decreases with the area of the opening; this again is mainly a dynamic effect created by a change in the period ratio, τ/T, of the loading which is introduced by the change of the system natural frequencies when the leak area is altered. The third point is indicative of the substantial coupling of the sub-systems in the overall motion. Had either been dominant the frequency of the pressure would have been that of the dominant sub-system. As it is, the frequency is neither that of the plate nor the leak; it is a beating combination of the two frequencies. This is illustrated for the 2,500 sq. inch opening in Fig.17(c) for which the two constituent pressure components are also drawn.

DISCUSSION

The finite element approach outlined in this chapter is perfectly general and may be applied to a structure of any shape provided this may be realised by an assemblage of finite elements and provided the maximum dimensions of the enclosed volume is small compared with the acoustic wavelength. The method has been applied to simple plate configurations because the results are tractable and of practical importance for window-room systems. No exact solutions are available for comparison purposes, though it is easy to obtain a series solution for the simply supported plate case, as illustrated in the introductory section.

For the free vibration the general trend of the natural frequencies and mode shapes are in agreement with those given by Dowell and Voss (4) and (5) who first assumed that the structural modes were uncoupled (4) and later (5) showed in a two mode approximation that the coupling between the modes is important at high values of η. Similar results were obtained by Pretlove (2) who obtained an exact solution for a one-dimensional beam-cavity model. In a sense, though, Pretlove's model was a little unrealistic for a plate system because the separation of the modes is greater for a beam; consequently the flattening effect on the $(\lambda/\lambda_{11}) \sim \eta$ curve did not occur until much higher values of η than those indicated in Fig. 8. However, both Dowell and Voss, and Pretlove gave experimental results (from a simple panel cavity model) which are in general agreement with those shown in Fig. 8.

As far as the author is aware no time domain solutions for the forced transient motion of plate-cavity systems have been given in the relevant literature. The results presented in the previous section for the plate motion and internal pressure do agree qualitatively with some of the field test results carried out at Edwards Air Force Base (10). Here the internal pressures of a window garage structure was at the same frequency as the window strain, as it would be for a sealed cavity.

The plate response parameters computed were displacements, velocities and accelerations; no attempt was made to evaluate the stresses. The cubic representation of the element displacement is equivalent to a linear variation for the stresses, because these involve the second spatial derivatives; hence a greater number of elements would be necessary to obtain the same degree of accuracy. For a large number of cases, though, the time histories of the stresses are similar to those of the displacements, with an added contribution from the higher modes. The displacements of a plate under a fixed loading decrease with the volume of the cavity - the acoustic and mechanical stiffnesses acting in parallel - and the mean displacement $\bar{d}$ may be obtained, approximately, for small values of η from the relationship:

$$\bar{d}_{cav} = \bar{d}/(1 + \eta).$$

However, as η increases the influence of the higher modes is more significant and although the mean displacements decrease there is an increase in the curvature and thus the stresses do not follow the displacements.

The result that increased pressures can be induced inside the cavity with a large flexible window and/or an opening, is important from the subjective and structural viewpoints. The subjective results would be mitigated (though the low frequency components may be amplified) as the most important high frequency components have been filtered out. However, minor structures which are so small as not to influence the overall motion may be overloaded with the increased pressure. In deriving the pressure ratios, Fig. 17, the part of pressure doubling needs to be emphasised. This assumption is not truly valid in practice as there is not a perfect reflection from the surface of the structure due to its motion and the actual factor may be less than two.

CONCLUSIONS

The low frequency behaviour of a coupled plate-acoustic system has been studied using a finite element displacement technique. The principal effect of the acoustic system on the mechanical system is to act as an additional strain energy source which is proportional to the square of the volume displacement of the plate surface. When the equations

of motion are formulated this term generates an additional stiffness matrix for the plate which couples all of the available degrees of freedom.

Using the theory, two studies have been made: the first on the free vibration of a simple plate cavity system; the second on the forced transient motion of similar systems, with particular regard for the response to an ideal 'n' wave.

The acoustic term is most significant for large flexible plates and small cavities. Under these conditions the in-vacuo principal modes of the plate are strongly linked and there is an increase in the natural frequencies of the volume displacing modes, the increase being most noticeable in the lowest mode of the system.

In the forced motion two situations were considered; the first where the cavity was sealed and acted as a pure stiffness, the second where the cavity acted as a coupling between a plate and a Helmholtz leakage term. Because of the change in natural frequencies and mode shapes there was also a change in the nature of the response time history; this was due to the induced change in the loadings period ratio, i.e. ratio of duration to fundamental period, and, when the frequencies were brought closer together, to the more significant effects of the other modes. The leak opening can also alter the motion of the plate and although for a large opening the initial response oscillates at a higher frequency than the in vacuo and sealed cases, the ensuing motion is dominated by a leak mode which oscillates at a lower frequency.

PART II: COUPLED WINDOW-CAVITY RESPONSE USING PLATE AND ACOUSTIC FINITE ELEMENTS

INTRODUCTION

The work of this section is divided into two main parts: firstly with the formulation of the equations of motion of a coupled plate-acoustic system using plate and acoustic finite elements; secondly, with the solution of these equations in the time domain.

Most work on similar problems has been concerned with the eigenvalues and modes of a particular system: Foxwell and Franklin (11) and later Warburton (12) considered the effects of an acoustic field on the vibrations of a cylindrical shell; Pretlove (2) analysed the response of a simply-supported panel backed by an acoustic cavity. In each of these papers the structure was represented by a series of the in vacuo normal modes; the acoustics by an exact solution of the acoustic wave equation, the two subsystems being linked by the conditions of equilibrium at the acousto-plate interface.

A general treatment of coupled acousto mechanical systems has been given by Gladwell and Zimmerman (13): they showed that the problem could be formulated entirely in terms of displacements or in terms of "force-like" quantities, stresses or pressures. Gladwell (14) later found, when attempting to obtain an approximate solution, that it was extremely difficult, if not impossible, to represent the acoustic system in terms of displacements so that the condition for irrotational motion was satisfied. However, it was possible to adopt a pressure formulation and this was done by Mason (15) when deriving a three dimensional acoustic element.

Here a mixed finite element formulation of the problem is used, displacements for the plate and pressures for the acoustics. Although this complicates the eigenvalue problem because the resulting overall system matrices are unsymmetric it does not cause any extra difficulty with the transient solution which is the main requirement. There is, in fact, some advantage in this mixed formulation when a comparison is to be made with experimental results, as mechanical measurements usually involve displacements or its time derivatives, acoustic measurements are usually pressures. Before computing the time domain response an eigenvalue solution for a simple hard walled room is carried out to test the accuracy of the acoustic elements in the frequency domain. The time domain response for a coupled system to an ideal 'n' wave is then given and a comparison is made between the responses for idealisations involving 2, 4 and 6 cuboid acoustic elements and a simple one-dimensional model

involving only acoustic plane waves. The effect of varying the depth of the cavity is considered using the 4 element model.

VARIATIONAL FORMULATION FOR THE EQUATIONS OF MOTION

Because of the restriction of the acoustic Lagrangian it is convenient first to divide the system into two parts: dealing with the mechanical subsystem in terms of displacements and then with the acoustics in terms of a velocity potential, ϕ. The two subsystems are then linked together through equilibrium considerations.

The action integral for the plate system assuming no prescribed motion at the boundaries is:

$$J = \int_{t_1}^{t_2} (TE_p - VE_p + (BE_E - BE_A))dt \qquad (25)$$

where TE_p is the kinetic energy; VE_p is the strain energy; BE_E is a term such that its variation δBE_E gives the work done by the external forces in a virtual displacement. BE_A is a similar term; the variation δBE_A gives the virtual work done by the acoustic back pressure. BE_A has a negative sign because it resists the motion impressed by the external load. When Hamilton's principle is applied, this gives the equation of motion for the plate:

$$\rho h\ddot{w} + \frac{Eh^3}{12(1-\mu^2)} \nabla^4 w = p_E(x,y,t) - p_A(x,y,t) \qquad (26)$$

The action integral for the acoustic system with a prescribed motion at a surface is

$$J^* = \int_{t_1}^{t_2} (TE_A^* - VE_A^* + BE_A^*)dt \qquad (27)$$

$$BE_A^* = BE_A.$$

The asterisk denotes that the respective energies are expressed in terms of velocity potential or pressures. BE_A^* is then such that its

variation δBE_A^* gives the complementary work done by the virtual forces at the acousto-mechanical interface. Since BE_A^* is equal to BE_A (and as they have opposite signs in equations (25) and (27)) these terms disappear in the Lagrangian for the overall coupled system.

Making JE* stationary gives the acoustic wave equation

$$\nabla^2\phi - \frac{1}{c^2}\frac{\partial^2\phi}{\partial t^2} = 0$$

with the dynamic boundary condition at the plate interface:

$$\rho\dot{w} = -\frac{\partial\phi}{\partial n}$$

where n denotes the direction of outward going normal.

The required formulation in terms of pressures is obtained by differentiating the latter equations with respect to time and applying the identity $p = -\rho(\partial\phi/\partial t)$. This gives the equations

$$\nabla^2 p - \frac{1}{c^2}\frac{\partial^2 p}{\partial t^2} = 0 \qquad (28)$$

$$\rho\ddot{w} = -\frac{\partial p}{\partial n} \quad \text{at the interface.}$$

An analytical solution of the equations (26) and (28) is extremely complicated for the general case. However, since the two integrals (25) and (27) give the correct equations of motion and dynamic boundary conditions they can be used as a basis for an approximate numerical solution.

Approximate Formulation of the Equations of Motion

In this section a finite element method is used to formulate the equations of motion for both the mechanical and acoustic subsystems. In each case the resulting equations are inhomogeneous. For the acoustic system the dynamic boundary condition at the interface is implied in a "generalised source" term on the right hand side of the equations.

Acoustic considerations.-

The potential energy $VE = \frac{1}{2}\rho c^2 \iiint (\text{div } u)^2 dxdydz$

where u is the particle displacement.

The kinetic energy, $TE = \frac{1}{2}\rho \iiint \dot{u}^2 \, dxdydz$

The work function, $BE_A = \iint p_A \, u \, dxdy$ at the interface.

These quantities may be rewritten in terms of the velocity potential by making use of the following relationships

$$\dot{u} = - \text{grad } \phi$$

$$\text{div. } u = - \frac{1}{c^2} \frac{\partial \phi}{\partial t}$$

$$p = -\rho \frac{\partial \phi}{\partial t}.$$

The action integral, equation (27) then becomes

$$JE^* = \int_{t_1}^{t_2} \{ \tfrac{1}{2}\rho \iiint (\text{grad } \phi)^2 dxdydz - \tfrac{1}{2} \frac{\rho}{c^2} \iiint \dot{\phi}^2 \, dxdydz + \iint (-\rho \dot{\phi}_s u_s) dxdy \} dt \qquad (29)$$

where the term in the curly brackets is the acoustic Lagrangian. It is this function which is to be approximated.

The approximate equations for a cuboid acoustic element.- Here a cuboid acoustic element is considered. The velocity potential throughout the element is described by means of the Hermitian interpolation polynomials, which were defined in Part I, and the four unknowns ϕ, $\partial\phi/\partial x$, $\partial\phi/\partial y$, $\partial\phi/\partial z$ at each corner of the element.

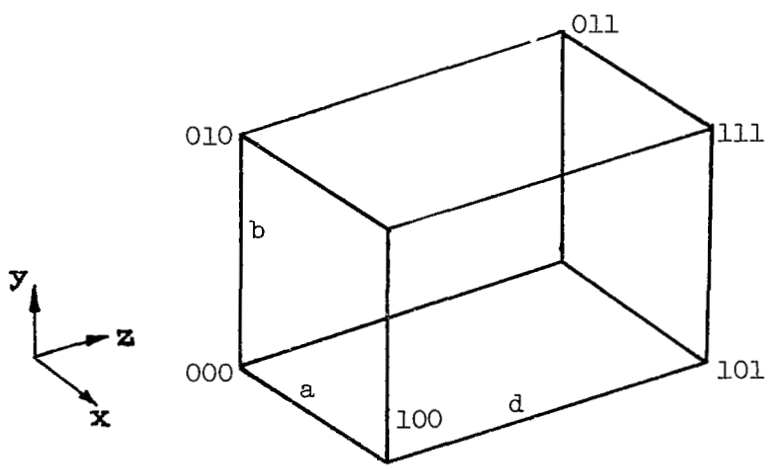

Cuboid Acoustic Element

$$X = \frac{x}{a}$$

$$Y = \frac{y}{b}$$

$$Z = \frac{z}{d}$$

At any point within the element boundaries the velocity potential is given by

$$\phi(x,y,z) = \phi_{000} g_1(X)g_1(Y)g_1(Z) + \frac{\partial\phi}{\partial z}_{000} g_2(X)g_1(Y)g_1(Z) + \frac{\partial\phi}{\partial y}_{000} g_1(x)g_2(Y)g_1(Z)$$
$$+ \frac{\partial\phi}{\partial z}_{000} g_1(X)g_1(Y)g_2(Z) + \phi_{010} g_1(X)g_3(Y)g_1(Z) + \frac{\partial\phi}{\partial x}_{010} g_2(X)g_3(Y)g_1(Z)$$
$$+ \frac{\partial\phi}{\partial y}_{010} g_1(X)g_4(Y)g_1(Z) + \frac{\partial\phi}{\partial z}_{010} g_1(X)g_3(Y)g_2(Z) + \phi_{100} g_3(X)g_(Y)g_1(Z)$$
$$+ \frac{\partial\phi}{\partial x}_{100} g_4(X)g_1(Y)g_1(Z) + \frac{\partial\phi}{\partial y}_{100} g_3(X)g_2(Y)g_1(Z) + \frac{\partial\phi}{\partial z}_{100} g_3(X)g_1(Y)g_2(Z)$$
$$+ \phi_{110} g_3(X)g_3(Y)g_1(Z) + \frac{\partial\phi}{\partial x}_{110} g_4(X)g_3(Y)g_1(Z) + \frac{\partial\phi}{\partial y}_{110} g_3(X)g_4(Y)g_1(Z)$$
$$+ \frac{\partial\phi}{\partial z}_{190} g_3(X)g_3(Y)g_2(Z) + \phi_{001} g_1(X)g_1(Y)g_3(Z) + \frac{\partial\phi}{\partial x}_{001} g_2(X)g_1(Y)g_3(Z)$$
$$+ \frac{\partial\phi}{\partial y}_{001} g_1(X)g_2(Y)g_3(Z) + \frac{\partial\phi}{\partial z}_{001} g_1(X)g_1(Y)g_4(Z) + \phi_{011} g_1(X)g_3(Y)g_3(Z)$$
$$+ \frac{\partial\phi}{\partial x}_{011} g_2(X)g_3(Y)g_3(Z) + \frac{\partial\phi}{\partial y}_{011} g_1(X)g_4(Y)g_3(Z) + \frac{\partial\phi}{\partial z}_{011} g_1(X)g_3(Y)g_4(Z)$$
$$+ \phi_{101} g_3(X)g_1(Y)g_3(Z) + \frac{\partial\phi}{\partial x}_{101} g_4(X)g_1(Y)g_3(Z) + \frac{\partial\phi}{\partial y}_{101} g_3(X)g_2(Y)g_3(Z)$$
$$+ \frac{\partial\phi}{\partial z}_{101} g_3(X)g_1(Y)g_4(Z) + \phi_{111} g_3(X)g_3(Y)g_3(Z) + \frac{\partial\phi}{\partial x}_{111} g_4(X)g_3(Y)g_3(Z)$$
$$+ \frac{\partial\phi}{\partial y}_{111} g_3(X)g_4(Y)g_3(Z) + \frac{\partial\phi}{\partial z}_{111} g_3(X)g_3(Y)g_4(Z)$$

This can be written in a reduced matrix form similar to that for the plate finite element:

$$\phi(x,y,z,t) = \{\phi_e(t)\}^T\{g_X g_Y g_Z\} \qquad (30)$$

From Part I the plate element displacement is

$$w(x,y,t) = \{w_e(t)\}^T\{f_X f_Y\}$$

The functions g_i and f_i are identical. Different symbols have been

adopted simply to differentiate between the plate and acoustic terms. Assuming that the displacement is prescribed in the x,y plane as in the shaded area on the above figure then the Lagrangian for the element is given by:

$$L = TE^* - VE^* + BE^*_A$$

where

$$TE^* = \tfrac{1}{2}\rho\{\phi_e\}^T \iiint \{g'_X g_Y g_Z\}\{g'_X g_Y g_Z\}^T + \{g_X g'_Y g_Z\}\{g_X g'_Y g_Z\}^T + \{g_X g_Y g'_Z\}\{g_X g_Y g'_Z\}^T \; dxdydz\{\phi_e\}$$

$$VE^* = \tfrac{1}{2}\frac{\rho}{c^2}\{\dot{\phi}_e\}^T \iiint \{g_X g_Y g_Z\}\{g_X g_Y g_Z\}\; dxdydz\{\dot{\phi}_e\}$$

$$BE^*_A = -\rho\{\dot{\phi}_e\}^T \iint \{g_X g_Y g_{Z=0}\}\{f_X f_Y\}^T \; dxdy\{w_e\}$$

The integral terms in the first two equations are square symmetric matrices and because there are the same number of displacement unknowns as velocity potential unknowns at the interface the surface integral term in the third equation is also square but not symmetric. The Lagrangian can then be re-written in an obvious notation as:

$$L = \tfrac{1}{2}\rho\{\phi_e\}^T[S_e]\{\phi_e\} - \tfrac{1}{2}\frac{\rho}{c^2}\{\dot{\phi}_e\}^T[P_e]\{\dot{\phi}_e\} - \rho\{\dot{\phi}_e\}^T[\theta_e]\{w_e\}$$

The equations of motion are now formed by making the action integral stationary for all arbitrary variations of the velocity potential which satisfy the kinematic boundary conditions and wnich also satisfy the condition

$$\{\delta\phi_e\} = \{0\} \quad \text{at} \quad t = t_1 \quad \text{and} \quad t = t_2.$$

$$\delta JE^* = \int_{t_1}^{t_2} \rho\{\delta\phi\}^T[S_e]\{\phi\} - \frac{\rho}{c^2}\{\delta\dot{\phi}\}^T[P_e]\{\dot{\phi}\} - \rho\{\delta\dot{\phi}\}^T[\theta_e]\{w\}dt = 0$$

After integrating the second and third terms by parts

$$\delta JE^* = \int_{t_1}^{t_2} \{\delta\phi_e\}^T\left[\rho[S_e]\{\phi\} + \frac{\rho}{c^2}[P_e]\{\ddot{\phi}\} + \rho[\theta_e]\{\dot{w}\}\right] dt = 0.$$

Since $\{\delta\phi\}$ is arbitrary then for this equation always to be true,

$$\rho[S_e]\{\phi\} + \frac{\rho}{c^2}[P_e]\{\ddot{\phi}\} - \rho[\theta_e]\{\dot{w}_e\} = 0$$

which is the approximate equation of motion for the acoustic element. It can be written in terms of the pressure vector by differentiating with respect to time and using the relationship $P = -\rho \frac{\partial \phi}{\partial t}$ giving

$$\frac{1}{\rho c^2}[P_e]\{\ddot{P}_e\} + \frac{1}{\rho}[S_e]\{P_e\} = [\theta_e]\{\ddot{w}_e\}. \qquad (31)$$

The equation may be compared with the inhomogeneous wave equation with a volume source term, which is Morse (17) (page 313)

$$\frac{1}{c^2}\ddot{p} - \nabla^2 p = \rho \frac{\partial q_s}{\partial t} \qquad (32)$$

where q_s is the source strength in rate of volume input units so that the right hand side involves an "acceleration" term. The equations are similar apart from the minus sign in front of the second term on the right hand side of the equation (32). This is due to the manner in which the matrix S was formed and may be explained by expanding the first term of equation (29) by parts; which for a cube of air with no work done on the boundaries gives

$$\iiint (\frac{\partial \phi}{\partial x})^2 + (\frac{\partial \phi}{\partial y})^2 + (\frac{\partial \phi}{\partial z})^2 dxdydz = - \iiint \phi (\frac{\partial^2 \phi}{\partial x^2} + \frac{\partial^2 \phi}{\partial y^2} + \frac{\partial^2 \phi}{\partial z^2}) dxdydz .$$

The S matrix, formed from the left hand side of this equation, was symmetric because of the quadratic form of the variables. Had it been formed from the right hand side the resulting matrix would have been unsymmetric but the sign would have been negative to conform with equation (31).

Equation (30) refers to the dynamics of a single element. The system equations for an assembly of these elements may be constructed in a similar manner to that described for the plate in the first section. For a system where the interface is in the xy plane, the final equation is of the form:

$$[P]\{\ddot{p}\} + [S]\{p\} = [\theta]\{\ddot{w}_b\} \qquad (33)$$

the suffix 'b' referring to the boundary displacements, where $[P]$ and $[S]$ are the relevant matrices for the overall system including the coefficients $1/\rho c^2$ and $1/\rho$ respectively.

It is of interest to note that the roles of the space and time derivatives are reversed when a 'force like' formulation is used. Here the kinetic energy is in terms of spatial derivatives and the strain energy in terms of the time derivatives.

Plate equations.- The essential details of this have been carried out in the first section. All that is required now is to derive an extra term to account for the acoustic back pressure. This is deduced from the variation of the quantity BE_A.

$$BE_A = \iint w.p.dxdy.$$

For a plate element on the face of an acoustic element, the face and plate having equal overall dimensions

$$BE_A = \{w_e\}^T \int\int \{f_X f_Y\}\{g_X g_Y g_Z=0\}^T \{P_e\}$$

$$= \{w_e\}[\theta]^T\{P_e\}.$$

The additional generalised force vector is given by $\{\frac{\partial BE_A}{\partial w_{ei}}\}$ so that the final equation for the plate element is

$$[M_e]\{\ddot{w}_e\} + [K_e]\{w\} = \{F\} - [\theta]^T\{P_e\} \qquad (34)$$

The overall plate equation is identical with the suffix e left out.

The coupled equations of motion.- In what follows the principal equations of motion for the two subsystems are combined into a single matrix equation and then arranged into the standard form suitable for the step by step solution. Assuming that the system is excited through the applied load at the surface of the plate only, i.e. there are no acoustic source terms, then the two equations (33) and (34) may be put into the form:

$$[M]\{\ddot{w}\} + [K]\{w\} + [\theta]^T\{P_b\} = \{F\}$$

$$-[\theta]\{\ddot{w}_b\} + [P]\{\ddot{p}\} + [S]\{p\} = \{0\}.$$

These can be re-written as a single matrix equation,

$$\begin{bmatrix} M & 0 \\ -\theta & P \end{bmatrix} \begin{Bmatrix} \ddot{w} \\ \ddot{p} \end{Bmatrix} + \begin{bmatrix} K & \theta^T \\ 0 & S \end{bmatrix} \begin{Bmatrix} w \\ p \end{Bmatrix} = \begin{Bmatrix} F \\ 0 \end{Bmatrix} \qquad (35)$$

The solution of equation (35) will give the coupled motion of the complete system without making any simplifying assumptions about weak coupling. It should be noted that as a result of the mixed formulation the "mass" and "stiffness" matrices are unsymmetric and subsequently an eigenvalue problem based on the homogeneous equation could be awkward. However, the main object is to obtain a solution to the forced motion in the time domain which may be achieved after arranging the equations into the standard form.

$$\{\dot{w}\} = \underset{\sim}{G}(w, \dot{w}, t).$$

This first requires the inversion of the "mass" matrix which is achieved by partitioning the unknown inverse matrix first into a compatible form. The inverse "mass" matrix is

$$\begin{bmatrix} M^{-1} & 0 \\ P^{-1}\theta M^{-1} & P^{-1} \end{bmatrix}$$

providing $[M]$ and $[P]$ are non-singular.

The standard form for the step by step solution is then:

$$\begin{Bmatrix} \dot{w} \\ \dot{p} \end{Bmatrix} = -\begin{bmatrix} M^{-1} & 0 \\ P^{-1}\theta M^{-1} & P^{-1} \end{bmatrix} \begin{bmatrix} K & \theta^T \\ 0 & S \end{bmatrix} \begin{Bmatrix} w \\ p \end{Bmatrix} + \begin{bmatrix} M^{-1} & 0 \\ P^{-1}\theta M^{-1} & P^{-1} \end{bmatrix} \begin{Bmatrix} F \\ 0 \end{Bmatrix} \tag{36}$$

The conciseness of the matrix form conceals an important factor: even for a small number of acoustic elements the number of simultaneous equations to be solved can be quite large and hence involve large amounts of computing time in their solution. Any means of reducing the computation should be used and it was solely for this reason that damping effects were neglected.

EIGENVALUE SOLUTION FOR THE ACOUSTIC ELEMENTS

The eigenvalue problem is important, particularly when the results may be compared with an exact solution as they then illustrate the degree of accuracy available with the approximate solution. As far as the author is aware no eigenvalue problem involving the acoustic finite elements described in equation (30) has been solved. The details of this element were given by Mason (15) but no computations were made. However, Mason did give the frequencies for a cuboid acoustic element constructed from different polynomial functions but with the same unknowns at each corner.

Assuming the homogeneous form of equation (33) and a time dependence of the form $\sin \omega t$ the required equation is

$$[S - \omega^2 P]\{p\} = 0 .$$

Two different configurations were considered when obtaining a solution; the first was made up of a column of equal elements as in Fig. 18(a), a different number of elements being used for various idealisations; the second system was made up from eight equal elements as shown in Fig. 18(b).

In both of these models the external boundaries were assumed to be hard so that, $\partial p/\partial \bar{n} = 0$, at the surfaces. Under these conditions there can be a static uniform pressure increase which is analogous to a rigid body mode in a mechanical system. In either case there is a zero natural frequency, which in the acoustic system implies that the matrix S is singular, and the singularity has to be removed before attempting to evaluate the other eigenvalues. This is done by 'constraining' the rigid body mode out of the equations of motion: a special subroutine for achieving this end has been written by Mason (15). The final order of the matrices involved is then reduced by one.

The Computed Eigenvalues and Eigenvectors

The computations were carried out on a system with dimensions 10" x 15" x 20"; for convenience the velocity of sound was put equal to unity. The results were then compared with the exact solutions:

eigenvalues $$\lambda^2_{\ell mn} = \pi^2\left(\frac{\ell^2}{a^2} + \frac{m^2}{b^2} + \frac{n^2}{d^2}\right)$$

eigenvectors $$\phi_{\ell mn} = \cos \frac{\ell \pi x}{a} \cos \frac{m \pi y}{b} \cos \frac{n \pi z}{d}$$

a, b and d are the cavity dimensions.

The results for the first seven modes using only a single element are shown in the table below. Even for this case the values are all within 0.13% of the exact solution, where the modes were adequately represented.

First seven eigenvalues obtained using one element

Mode	0,0,1	0,1,0	0,1,1	1,0,0	1,0,1	1,1,0	1,1,1
Exact x 10^{-2}	2.4674	4.3865	6.8539	9.8696	12.337	14.256	16.723
Computed x 10^{-2}	2.4706	4.3922	6.8628	9.8824	12.353	14.275	16.745
% error	.125	.130	.113	.130	.121	.126	.130

With a single element the (0,0,2) mode has the same eigenvalue as the (1,0,0) mode but, because there are insufficient degrees of freedom available the eigenvalue for the (0,0,2) mode is not computed.

Fig.19 shows the accuracy and convergence of the eigenvalues for the (0, 0, 1), (0, 0, 2) and (0, 0, 3) modes as the number of elements is increased. The curves show that there is monotonic convergence to the exact solution in each case. When six elements are used the accuracy of the computed value comes into the limits specified in the eigenvalue routine (+0.001%) so the points below this value should be treated with caution.

The accuracy of the eigenvalues implies that there is a good approximation to the true mode shapes by the assumed polynomial functions. When the modes were computed only the values at the node points were printed out, and, in the single element case, the values for the first seven modes are shown below. The numbers refer to the pressure with the locations shown in the diagram. All the space derivatives are zero.

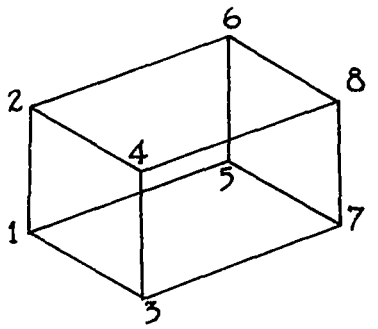

Mode	Position							
	1	2	3	4	5	6	7	8
0,0,1	+1	+1	+1	+1	-1	-1	-1	-1
0,1,0	-1	+1	-1	+1	+1	-1	+1	-1
0,1,1	-1	+1	-1	+1	-1	+1	-1	+1
1,0,0	-1	-1	+1	+1	-1	-1	+1	+1
1,0,1	-1	-1	+1	+1	+1	+1	-1	-1
1,1,0	-1	+1	+1	-1	-1	+1	+1	-1
1,1,1	+1	-1	-1	+1	-1	+1	+1	-1

There is insufficient information here to check the detailed mode shape; this would have to be evaluated using the polynomial expression in equation (30). Since the actual modes involve separable functions in x, y and z, the essential qualities of the approximation may be obtained by considering only one direction. For a plane wave mode which may be the (0,0,1), (0,1,0) or (1,0,0) mode the function is simply:

$$\phi(\varepsilon) = g_1(\varepsilon) - g_3(\varepsilon)$$
$$= 1 - 6\varepsilon^2 + 4\varepsilon^3.$$

The results for five intermediate positions are compared with the exact solution below and it may be seen that the results are quite accurate.

Exact	1.000	.866	.500	0.000	-.500	-.866	-1.000
1 element	1.00	.852	.481	0.000	-.481	-.852	-1.000

Much greater accuracy is obtained with a larger number of elements and the normalised modes for the first 3 eigenvalues were all correct to three decimal places when six finite elements were used.

The study on the column system was made to examine the convergence qualities when the number of acoustic elements in one direction was increased. Restricting the increased flexibility in this manner brings out the salient features without over increasing the size of the matrices and subsequently the computation time. However, the elements are to be applied to a more general situation when dealing with the forced vibration and it is important to know the order of accuracy when there is equal flexibility in all directions. In view of the stability criteria for the step by step procedure, Craggs (9), it was particularly important to know the behaviour of the highest eigenvalue. It was with these points in mind that the configuration of Fig. 18(b) was considered.

The results are shown in Table 1 where the modes have been classified into eight different groups corresponding to whether they were symmetric or anti-symmetric in the x, y and z directions. Again the lowest eigenvalues are extremely accurate and even the highest - the 56th - is estimated to within 6%, so that the highest frequency was correct to within 3%. However, there is an error of 15% in the eigenvalue of the 21st mode and with four other modes the error is greater than 10%. These errors always occur in the modes for which ℓ, m or n is 3 and the particular modes consequently need a larger number of elements to give a better representation.

Discussion.- In the above the acoustic elements have been tested in the frequency domain and the results bring out two important factors: the accuracy of the eigenvalues implies that the strain and kinetic energies are adequately represented at least for the simple models considered; but more important, is the result that the solutions have monotonic convergence to the exact solution. The element tested by Mason gave comparable accuracy with a small number of elements, but when the number was increased the values diverged from the exact solution.

The application of the acoustic element discussed here together with

the plate element developed by Mason which is described in Part 1, should give reliable solutions for the frequency domain solution of the coupled system. The accuracy is needed more with the acoustics though, even at the low frequency end of the spectrum, because the modal density is high and, unlike the plate system, a large number of modes can participate in the motion for a transient disturbance.

The remaining part of this section is concerned with the numerical solution of the coupled equations of motion in the time domain.

THE TRANSIENT FORCED VIBRATION OF THE COUPLED SYSTEM

A detailed description complete with subroutine listings is given in Craggs (16). The programme was written so that it could deal specifically with the type of model described in the next section, and no attempt was made to deal with the general case.

The general layout of the programme is as follows:

Stage 1 (a) Form unconstrained plate mass and stiffness matrices.
(b) Apply appropriate constraints.
Stage 2 (a) Form unconstrained P and S matrices.
(b) Apply constraints.
Stage 3 (a) Form θ^T matrix.
(b) Remove rows corresponding to mechanical constraints.
(c) Remove columns corresponding to acoustic constraints.
Stage 4 Assemble overall system equations.
Stage 5 Solve equations for different force vector at each step.

In common with the plate equations described in Part 1, it was found necessary to introduce an appropriate scaling factor in order to avoid numerical overflow. The equations which were set up for solution were in the form:

$$\begin{bmatrix} M & 0 \\ \varepsilon\theta & P \end{bmatrix} \begin{Bmatrix} \ddot{w} \\ \ddot{p} \end{Bmatrix} + \begin{bmatrix} \varepsilon K & \theta^T \\ 0 & \varepsilon S \end{bmatrix} \begin{Bmatrix} w \\ p \end{Bmatrix} = \begin{Bmatrix} F \\ 0 \end{Bmatrix}$$

where ε is the scaling factor (again a suitable value was 10^{-6}). The true solutions of this equation were derived from

$$\{w\}_{actual} = \varepsilon\{w\}_{computed}; \quad \{P\}_{actual} = \{P\}_{computed}$$

$$\text{actual time} = \text{computed time} \times \sqrt{\varepsilon}.$$

RESULTS

The aims of the computations were: first to examine the approximate solution in the time domain and compare this with an exact solution where this was possible; secondly, to note the change, if any, in the response parameters when further degrees of freedom were introduced by considering more acoustic elements. Most of the computed results refer to a simple window-room structure of window dimensions 120" x 60" x 0.25", and cavity of dimensions 120" x 120" x 198". In order to consider further effects of an acoustic standing wave the depth was varied from 58" to 600".

Four computer models were used: the first three were the same plate system with a different number of three dimensional acoustic elements; the fourth model was constructed by considering three plate normal modes and four one dimensional acoustic elements. These elements allowed only a plane wave acoustic disturbance in a direction perpendicular to the face of the plate; they made a great saving in computing time at the expense of flexibility.

In all cases the excitation was assumed to take place at normal incidence and have the form of an ideal 'n' wave and since the three-dimensional models were symmetric it was expedient to use this property to reduce the size of the working matrices by a procedure which is described in Appendix 1. The details of the reduced finite element models are shown in Fig. 20; also shown on the figure are the number of degrees of freedom available. It will be noticed that only a single plate element is used which in this case is equivalent to four elements. Reducing the system in this way eliminates the redundant degrees of freedom, that is those modes which are not excited under normal incidence conditions. The number of acoustic elements is also equivalent to four times the number used as the system is symmetric about the neutral axis. The details of the constraints on both the plate and acoustic systems to achieve these reduced forms are given in Appendix 1.

Basic check results.- In the exact solution the equilibrium at the acoustic mechanical interface demands that $\rho\ddot{w} = -\partial p/\partial z$ be satisfied over the entire surface of the plate. Because both systems are effectively constrained to move in a finite number of modes, this condition cannot be achieved. However, the variational principle should produce a result for minimum error. Fig. 21 shows the values of $\rho\ddot{w} \sim \partial p/\partial z$ at the centre of the plate. It may be seen that the two curves each have a different high frequency oscillation corresponding to motion in the higher modes of each subsystem. The low frequency curve - or the mean curve drawn through the high frequency oscillation term - almost complies with the requirement for equilibrium.

Fig. 22 shows the initial motion of the acoustic system and gives a

comparison between the pressures at the plate surface, the centre of the room, and the centre of the rear wall. Two points may be noticed: first, there is a high frequency component at the surface of the plate which diminishes along the length of the room, which suggests a cut-off type mode; second, the delay effect at each station is a good approximation to the exact delay time, z/c.

Results from the various models.- Some comparisons between the different models are given in Table 2. This table shows the maximum values of the window displacements and the room pressures just inside the window and at the back face. There is, in general, a close agreement between the indicated trends of all the models.

The salient features of the different models' pressure responses are shown in Fig. 23 where the pressure time histories from the models MAI, MAIII (see Fig. 20) and the plane wave model, each having a depth of 174", are compared for an 'N' wave duration of 200 milliseconds. Because no allowance for the cross modes was made with the plane wave model the time histories are much smoother.

Further response curves are shown in Fig. 24, these being computed with the model MAII for a cavity depth of 198".

With all of the acoustic pressure responses the main form of the time histories - principally that of the window displacement - are distorted by the contributions from a plane wave depth mode which propagates in the z-direction. This point is well illustrated in Fig. 24 which shows the pressure histories computed at different locations in the room for several 'n' wave durations; the shape of the acoustic mode concerned has the form

$$\frac{\cos \theta(\text{depth} - z)}{\text{depth}} \quad ; \qquad 0 < \theta < \frac{\pi}{2} .$$

In particular $\theta \doteqdot \frac{\pi}{4}$.

The effects of the cross modes are significant particularly near the surface of the window, the predominant frequency being of the order of 130 c.p.s. However, in the earlier phase of each response, higher frequency components are present. Away from the window the effects of these modes are attenuated and they make little contribution to the overall pressure on the back face.

The shock spectra of the window's displacement and velocity and the acoustic pressures, due to an ideal 'n' wave excitation are shown in Fig. 25. Again these refer to the model with a depth of 198" and were evaluated with the model MAII. As with the time histories the pressure shock spectra are of the same form as the displacement spectra and the maximum maxima occur at the same duration, this duration being equal to

the fundamental period of the window. An exception occurs with the spectra for the pressure at the window. Because of the influence of the acoustic depth mode, the pressure is much less than anywhere else in the cavity. The maximum pressures occur on the rear face.

It is of interest to observe that the pressures are of the order that is indicated by the volume displacement method discussed in Part 1, being given by:

$$\frac{p(\text{internal})}{p(\text{external})} = \frac{\eta}{(1 + \eta)} \cdot D$$

where D is a dynamic multiplier which varies from 0 to 2.1 depending upon the ratio - n wave duration/fundamental period of window.

The effect of cavity depth.- The results of this section serve two main purposes: first, to determine the effect on the system as the room changes from being a stiffness reactance to the plate - as for a shallow cavity - to an inertia reactance as for a long cavity. It also acts as another cross check on the performance of the model because the results may be compared with those indicated by the simple theory of the previous chapter.

The important points are brought out by varying the depth of the cavity and dealing only with the first half oscillation of the response parameters. The results, shown in Fig. 26, give the changes in the displacement and pressure responses. When the depth of the room is reduced (100", 50") the plate displacement decreases while there is an increase in the internal pressure. The frequency of oscillation which is governed by the plate motion also increases. When the depth is increased to 400" the cavity becomes strictly mass reactive relative to the plate; consequently the plate frequency decreases and the internal acoustic pressure no longer follows the form of the plate displacement.

The reasons for this behaviour may be given by making a simple idealisation of the system: representing the window by a spring-mass oscillator with a flat surface and allow only acoustic plane waves in the direction normal to the surface of the plate. In which case the frequency equation for the system is:

$$\tan\left(\frac{\omega \ell}{c}\right) = \frac{\rho \omega_c A}{(\omega^2 m - k)}$$

where ℓ is the depth of the cavity; A is the plate area; m is the plate mass; k the plate stiffness; ρ the density of the enclosed gas; c is the speed of sound. The roots for the various depths may be found graphically as shown in Fig. 27 which also shows the nature of the acoustic modes.

For the short depth the first acoustic mode indicates a near uniform pressure throughout the length of the room. In this situation the volume displacement stiffness applies and the increased acoustic stiffness, which reduces the plate response, is brought about by an increase in the acoustic pressure.

The acoustic situation completely changes with the larger depth: Fig. 26 shows that there are two modes close together both having a negative pressure component at the face of the plate for an inward plate displacement. This fact and the decrease in the plate frequency are characteristic of an inertia reactance. Because the frequency of the second mode is so close to that of the first mode it will be significant in the response, particularly in the initial stages, and this is shown to be the case in Fig. 26(b).

DISCUSSION AND CONCLUSIONS

In this part the acousto-mechanical problem has been treated approximately in terms of mixed force and displacement variables; this did not bring about any difficulties with the solution of the resulting equations to a transient excitation, even though the overall matrices involved were unsymmetric. The motion is governed by an equation (35). This result is of a general application and may be applied to any acousto-mechanical system whether the subsystems are idealised with finite elements or an assumed modes approach. Here plate and acoustic finite elements have been used when idealising the subsystems.

The acoustic elements give extremely accurate results; their chief disadvantage is that they involve a large number of degrees of freedom. However, this may be a necessary result for three dimensional problems because of the usual large modal densities. It is important to reduce the number of degrees of freedom where this is possible by removing the redundant variables. For the type of problem considered here this has been achieved by invoking symmetric properties of the system and loading; subsequently, the matrices involved have been reduced to one quarter their original size. The simple one-dimensional model gave adequate results; though, of course, its application is restricted to the case where the plate wave motion is dominant.

No exact solutions for the time histories of the forced transient motion of a coupled acousto-mechanical system are available. However, the results do comply with the volume displacing theory results where these were applicable; they also comply with the analytical results deduced from a plane wave model coupled to a simple oscillator, so that the computer program appears to be working satisfactorily.

An interesting point which is brought out in the three-dimensional model is that the pressure has high frequency components near the window face. This result is important when dealing with a subjective evaluation of the room response. When the room is not shallow the acoustic effects on the window are negligible; nowhere in the results do the acoustic oscillations lead to a build up in the plate motion, they always act to suppress it.

APPENDIX 1

Reduction of the Problem Size by Applying Properties of Symmetry

Throughout the latter half of this report use has been made of the symmetrical properties of a particular system to reduce the size of the problem. In the two dimensional cases studied the size of the matrices involved have been reduced by a factor of four; in one three dimensional case there was a reduction by a factor of eight. When dealing with forced motion it is also required to have a symmetric pressure distribution as well as symmetric mass and stiffness properties. Here a discussion on the application of symmetry is given. This is followed by the details of the relevant symmetry constraints which were applied to the various systems mentioned in the main text.

For simplicity consider a two-dimensional system in the x,y plane. The equation of motion is

$$M\ddot{w} + Kw = F. \tag{A1}$$

If the system is symmetric in both the x and y directions then it may be divided into four parts each part having a corresponding displacement and loading vector. Now, if the equations of motion of each section are rearranged so that the displacements in each section are in order:

$$\underset{\sim}{w}_1 = \underset{\sim}{w}_2 = \underset{\sim}{w}_3 = \underset{\sim}{w}_4,$$

and the forces

$$\underset{\sim}{F}_1 = \underset{\sim}{F}_2 = \underset{\sim}{F}_3 = \underset{\sim}{F}_4 \tag{A2}$$

then the equation for the whole system (A1) may be reproduced in a partitioned form:

$$\begin{bmatrix} M_{11} & M_{12} & M_{13} & M_{14} \\ M_{21} & M_{22} & M_{23} & M_{24} \\ M_{31} & M_{32} & M_{33} & M_{34} \\ M_{41} & M_{42} & M_{43} & M_{44} \end{bmatrix} \begin{bmatrix} \ddot{\underset{\sim}{w}}_1 \\ \ddot{\underset{\sim}{w}}_2 \\ \ddot{\underset{\sim}{w}}_3 \\ \ddot{\underset{\sim}{w}}_4 \end{bmatrix} + \begin{bmatrix} K_{11} & K_{12} & K_{13} & K_{14} \\ K_{21} & K_{22} & K_{23} & K_{24} \\ K_{31} & K_{32} & K_{33} & K_{34} \\ K_{41} & K_{42} & K_{43} & K_{44} \end{bmatrix} \begin{bmatrix} \underset{\sim}{w}_1 \\ \underset{\sim}{w}_2 \\ \underset{\sim}{w}_3 \\ \underset{\sim}{w}_4 \end{bmatrix} = \begin{bmatrix} \underset{\sim}{F}_1 \\ \underset{\sim}{F}_2 \\ \underset{\sim}{F}_3 \\ \underset{\sim}{F}_4 \end{bmatrix}$$

The suffices refer to the sections.

Multiplying this equation out gives four matrix equations. However, it is only necessary to consider one of them, thus:

$$M_{11}\ddot{\underset{\sim}{w}}_1 + M_{12}\ddot{\underset{\sim}{w}}_2 + M_{13}\ddot{\underset{\sim}{w}}_3 + M_{14}\ddot{\underset{\sim}{w}}_4 + K_{11}\underset{\sim}{w}_1 + K_{12}\underset{\sim}{w}_2 + K_{13}\underset{\sim}{w}_3 + K_{14}\underset{\sim}{w}_4 = \underset{\sim}{F}_1$$

applying (A2) gives

$$\left[M_{11} + M_{12} + M_{13} + M_{14}\right]\underset{\sim}{\ddot{w}}_1 + \left[K_{11} + K_{12} + K_{13} + K_{14}\right]\underset{\sim}{w}_1 = \underset{\sim}{F}_1 .$$

This is the reduced equation for the system. It shows that the coupling matrices between each of the sections must be added together. However, with the usual in-vacuo finite element formulation the coupling between each of the sections is zero and the equation reduces to

$$M_{11}\underset{\sim}{\ddot{w}}_1 + K_{11}\underset{\sim}{w}_1 = \underset{\sim}{F}_1. \qquad \text{(A3)}$$

Plate equations: the equations for a plate may be deduced directly by imposing constraints for symmetry along the dividing edges as well as the fixed constraints.

For symmetry in the x direction, $\partial w/\partial y = 0$.
For symmetry in the y direction, $\partial w/\partial x = 0$.
For the corner which represents the plate centre, $\partial^2 w/\partial y \partial x = 0$.

When the volume displacement stiffness matrix is added to the mechanical stiffness matrix there is a cross coupling between the other segments. The stiffness terms for the reduced system is then:

$$K^M_{11}\underset{\sim}{w}_1 + \left[K^C_{11} + K^C_{12} + K^C_{13} + K^C_{14}\right]\underset{\sim}{w}_1.$$

The suffices M and C refer to mechanical and cavity terms respectively. But

$$K^C_{11} = K^C_{12} = K^C_{13} = K^C_{14}.$$

The stiffness terms are then

$$K^M_{11}\underset{\sim}{w}_1 + 4K^C_{11}\underset{\sim}{w}_1.$$

This means that the acoustic stiffness term must be increased four times, which really implies that the volume of the backing cavity is reduced by four.

Plate and Acoustic Finite Elements for MAI, MAII, MAIII.

The plate constraints are as above. The constraints on the acoustic elements at faces of symmetry in the x, z, and y, z planes only were:

x, z plane, $\partial p/\partial y = 0$
y, z plane, $\partial p/\partial z = 0$.

Acoustic Eigenvalue Problem.

In this case the system involving eight acoustic elements was reduced to one having only one element. The reduced size of the problem involved studying the single element configuration more times with different constraints at the planes of symmetry. This effectively meant treating the symmetric and antisymmetric modes in the x, y and z directions separately.

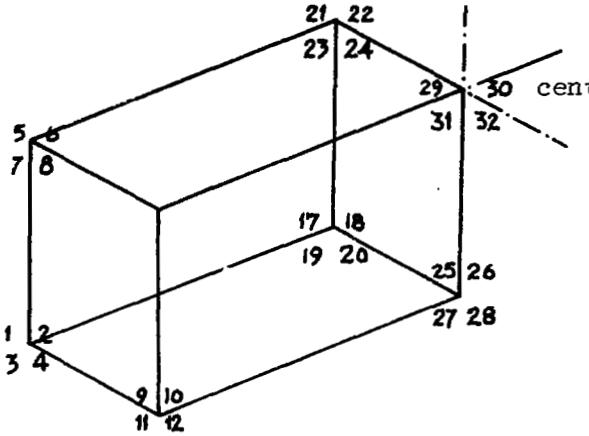

at each node the unknowns are

$$p, \frac{\partial p}{\partial x}, \frac{\partial p}{\partial y}, \frac{\partial p}{\partial z}$$

In the model the planes 1, 5, 21, 17; 1, 5, 13, 9; 1, 9, 25, 17 are always hard, the constraints being $\partial p/\partial \bar{n} = 0$. $\bar{n}$ denotes the outgoing normal.

On the other faces, 5, 13, 29, 21; 9, 13, 29, 25; and 1, 9, 25, 17 the constraints depend upon whether the mode shape in the x, y or z direction is symmetric or antisymmetric.

For symmetry $\partial p/\partial \bar{n} = 0$.

For antisymmetry p, $\partial p/\partial r$, $\partial p/\partial s = 0$, where the constraints are applied in the r, s plane.

Thus, there are eight combinations of modes and the appropriate constraints for each set are shown in the table which follows. The numbers refer to those shown in the diagram above.

Coordinate No,	1 2 3 4	5 6 7 8	9 10 11 12	13 14 15 16	17 18 19 20	21 22 23 24	25 26 27 28	29 30 31 32
Fixed Constraints	C C C	C C	C C	C	C C	C	C	
X Symmetric s			C	C			C	C
X Asymmetric a			C C C	C C C			C C C	C C C
Y Symmetric s		C		C		C		C
Y Asymmetric a		C C C		C C C		C C C		C C C
Z Symmetric s					C	C	C	C
Z Asymmetric a					C C C	C C C	C C C	C C C

Data for Symmetric and Asymmetric modes using only one element

Note: There are 8 cases expressed in the order (x,y,z). SSS, SSA, SAS, ASS, SAA, ASA, AAS, AAA.

REFERENCES

1. LYON, R.H. — Noise reduction of rectangular enclosures with one flexible wall. J. Acoust. Soc. Amer. 1963. 35. p.1791.
2. PRETLOVE, A.J. — The response of large windows to sonic bangs. J. Sound Vib. (to be published 1969).
3. PRETLOVE, A.J. — Free vibrations of a rectangular panel backed by a closed rectangular cavity. J. Sound Vib. 1965. 3, p.252.
4. DOWELL, E.H. VOSS, H.M. — The effect of a cavity on panel vibration. A.I.A.A. Jrnl. 1, 1963, p.476.
5. DOWELL, E.H. VOSS, H.M. — Theoretical and experimental panel flutter studies in the Mach number range 1.0 to 5.0. A.I.A.A. Jrnl, 3, 1965, p.2292.
6. LYON et al. — Low frequency noise reduction of spacecraft structures. N.A.S.A. CR-589, 1966.
7. MASON, V. — Rectangular finite elements for analysis of plate vibrations. J. Sound Vib. 1968, 7(3), p.437.
8. WARBURTON, G.B. — The vibration of rectangular plates. Proc. Inst. Mech. Eng. 1954. 168,p.371.
9. CRAGGS, A. — Transient vibration analysis of linear systems using transition matrices. N.A.S.A. CR-1237. 1968.
10. Interim Report — Sonic boom experiments at Edwards Airforce Base. National Sonic Boom Evaluation Office, Arlington, Virginia, 1967.
11. FOXWELL, J.H. FRANKLIN, R.E. — The vibrations of a thin-walled stiffened cylinder in an acoustic field. Aeronautical Quarterly, 1, 1959, p.47.
12. WARBURTON, G.B. — Vibration of a cylindrical shell in an acoustic medium J. Mech. Eng. Science, 1961, 3, p.69.
13. GLADWELL, G.M.L. ZIMMERMAN, G. — On energy and complementary energy formulations of acoustic and structural vibration problems. J. Sound Vib, 1966, 3, p.233.
14. GLADWELL, G.M.L. — A variational formulation of damped acousto-structural vibration problems. J. Sound Vib., 1966, 4, p.172.

15. MASON, V. On the use of rectangular finite elements. Institute of Sound and Vibration Research Report No. 161, 1967.

16. CRAGGS, A. The response of acousto-mechanical systems to sonic booms. Ph.D. Thesis, University of Southampton, 1969.

17. MORSE, P.M. Vibration and Sound. McGraw Hill, 1948.

18. CRAGGS, A. The response of a simply supported plate to transient faces. Part 1: The effect of N waves at normal incidence. NASA CR1175, September 1968.

TABLE 1

Percentage Error in Eigenvalues for Cuboid Acoustic System represented by Eight Elements

mode	S.S.S.		S.S.A		S.A.S.		S.A.A.		A.S.S.		A.S.A.		A.A.S.		A.A.A	
1	0.1297	4	0.0284	1	0.0274	2	1.0593	3	0.0263	4	0.999	6	1.0522	7	1.9076	9
2	0.1311	10	0.1199	12	0.0982	7	9.8071	15	0.0811	10	0.489	19	0.6715	14	15.2504	21
3	0.1277	16	6.1062	13	6.1072	23	7.6505	26	0.0912	16	13.340	20	10.7036	20	11.7148	34
4	0.1292	23	3.4664	25	0.1192	28	-4.8013	29	0.1019	22	8.671	33	8.8887	37	7.9327	51
5	0.1297	30	0.1240	26	4.8527	32	11.4209	39	6.1063	47	6.787	49	7.3168	50		
6	0.1298	36	0.1244	38	0.1135	35	4.0037	46	5.5015	52	5.714	56	6.6259	54		
7			0.0223	39	0.0302	44										

Note: S - symmetric; A - antisymmetric, define modes in x, y, z directions. The numbers in the right hand columns give the location of the mode in the frequency scale.

TABLE 2

Max. Values for Different Models

τ		$\hat{d}$	$\hat{p}(0)$	$\hat{p}(1)$
50 ms.	MAI	-.0946	-.1753	-.2742
	MAII			
	MAIII	-.0929	-.1770	-.289
100 ms.	MAI	-.1727	-.3080	-.4683
	MAII	-.1712	-.2865	-.4700
	MAIII	-.1725	-.2863	-.4743
200 ms.	MAI	-.1526	-.2826	-.4017
	MAII	-.1493	-.2463	-.3929
	MAIII	-.1504	-.2354	-.3992

Plane Wave Model

τ	$\hat{q}_{11}$	$\hat{p}(0)$	$\hat{p}(1)$
50 ms.	0.089	.174	.206
100 ms.	.176	.285	.368
200 ms.	.151	.222	.312

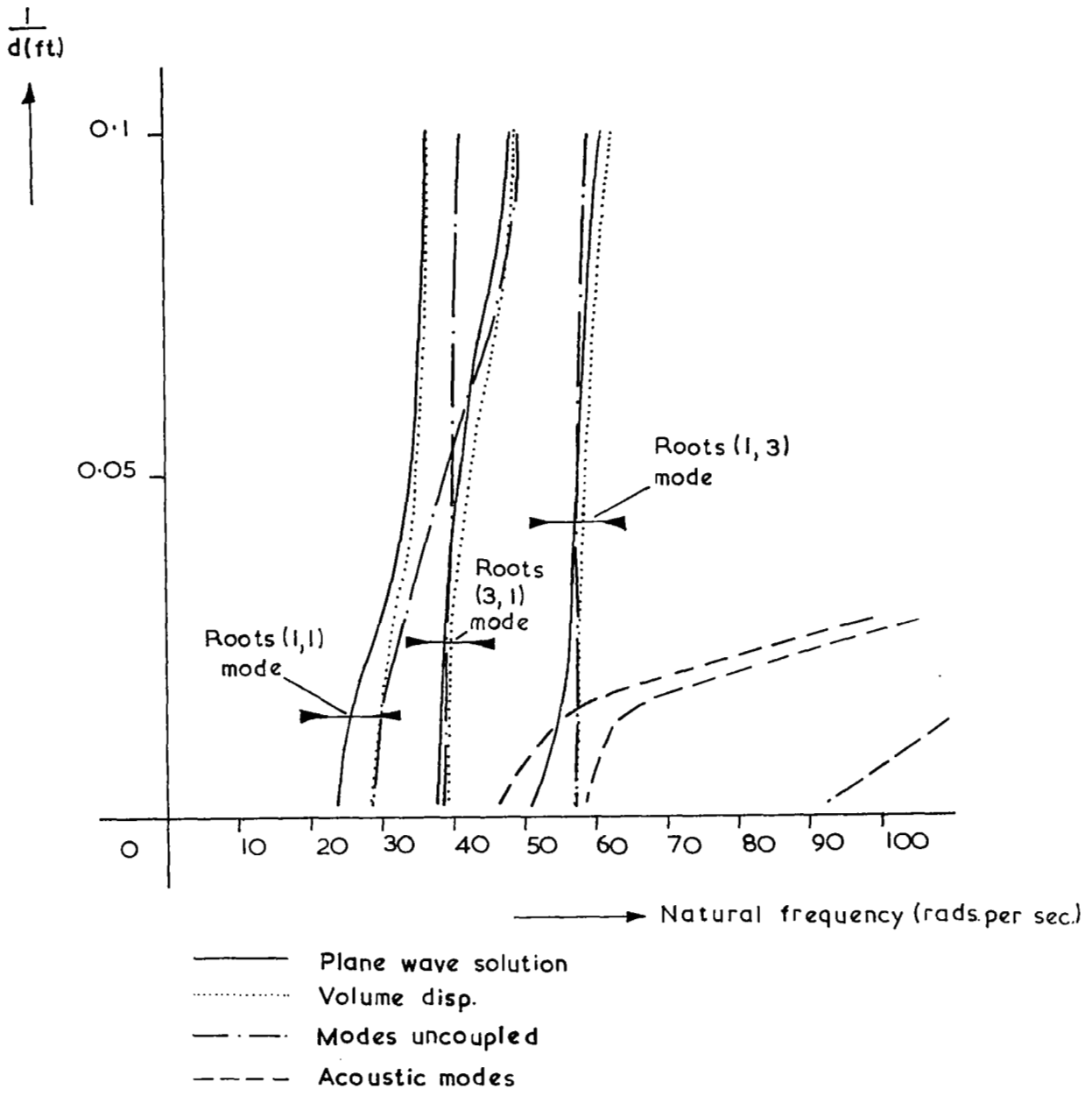

Fig 2 Comparison of Roots for Simple Plate Cavity System.

The first 3 in vacuo natural frequencies of plate are:

$\omega_1 = 23{\cdot}84$, $\omega_2 = 38{\cdot}50$, $\omega_3 = 56{\cdot}84$ (rads. per sec)

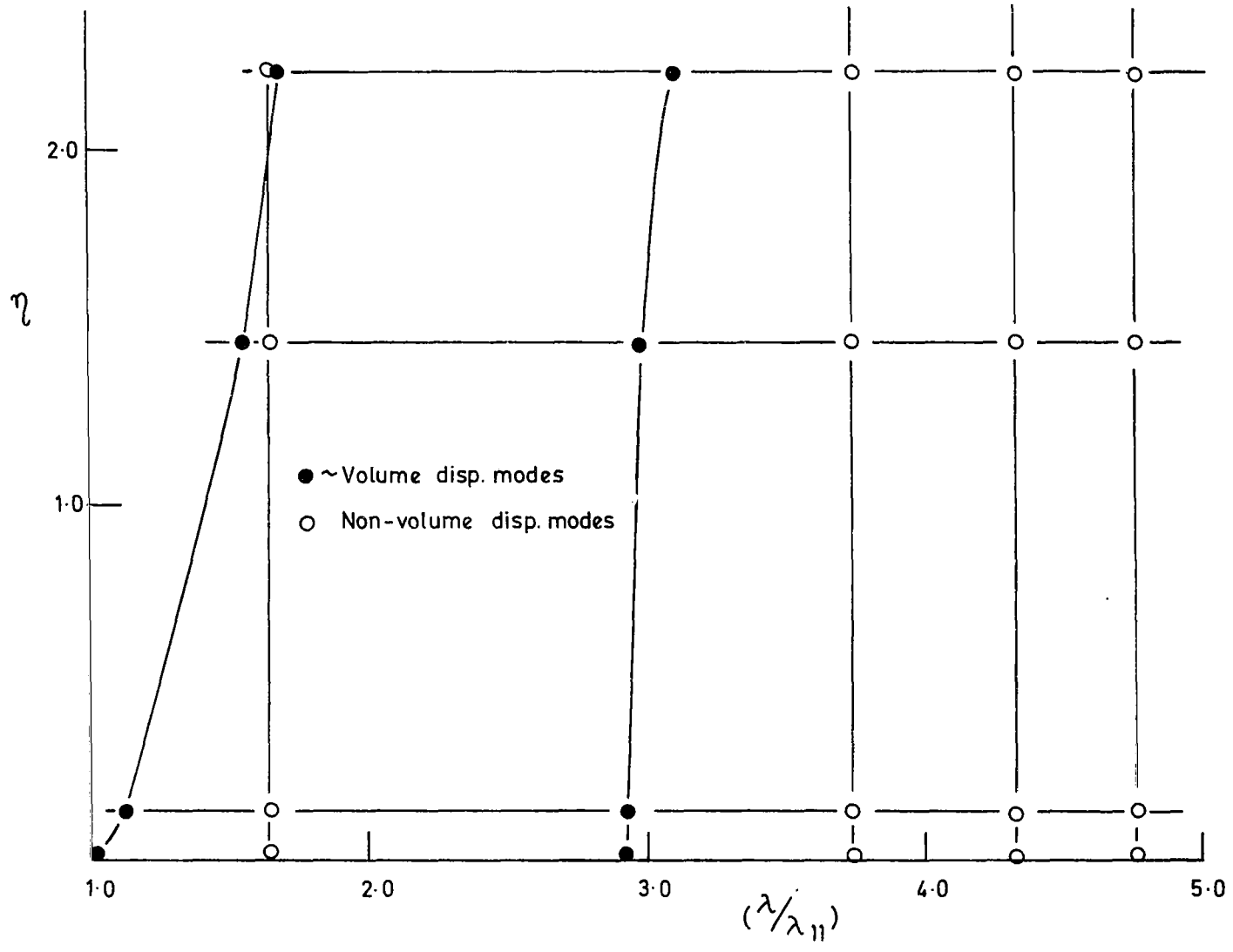

Fig. 3 Variation of natural frequencies $\sim \eta$ 4 element idealisation Simply supported plate , $\beta = 2{\cdot}0$

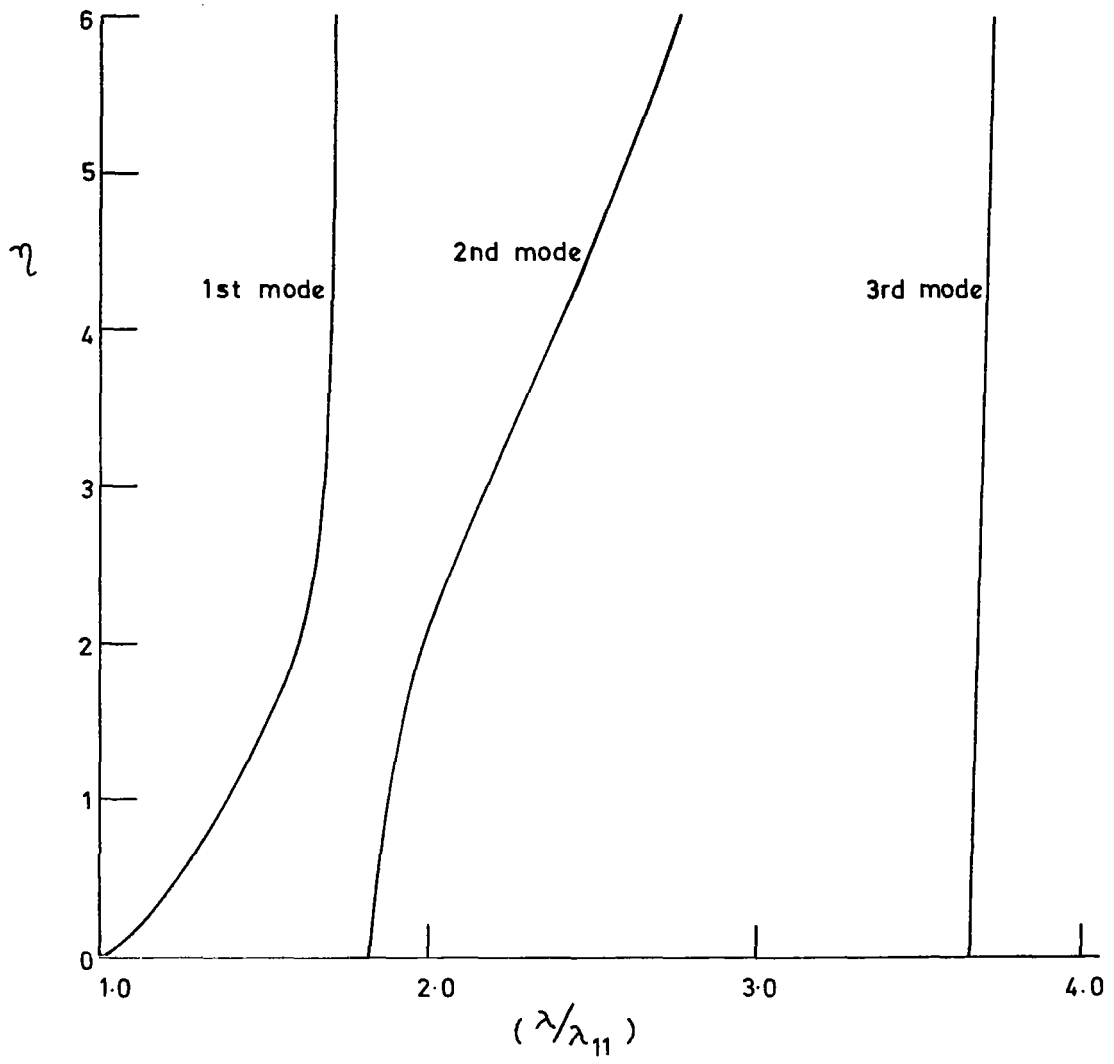

Fig. 4 Variation of natural frequencies ~ η
Simply supported plate, $\beta = 3{\cdot}0$, 16 element idealisation

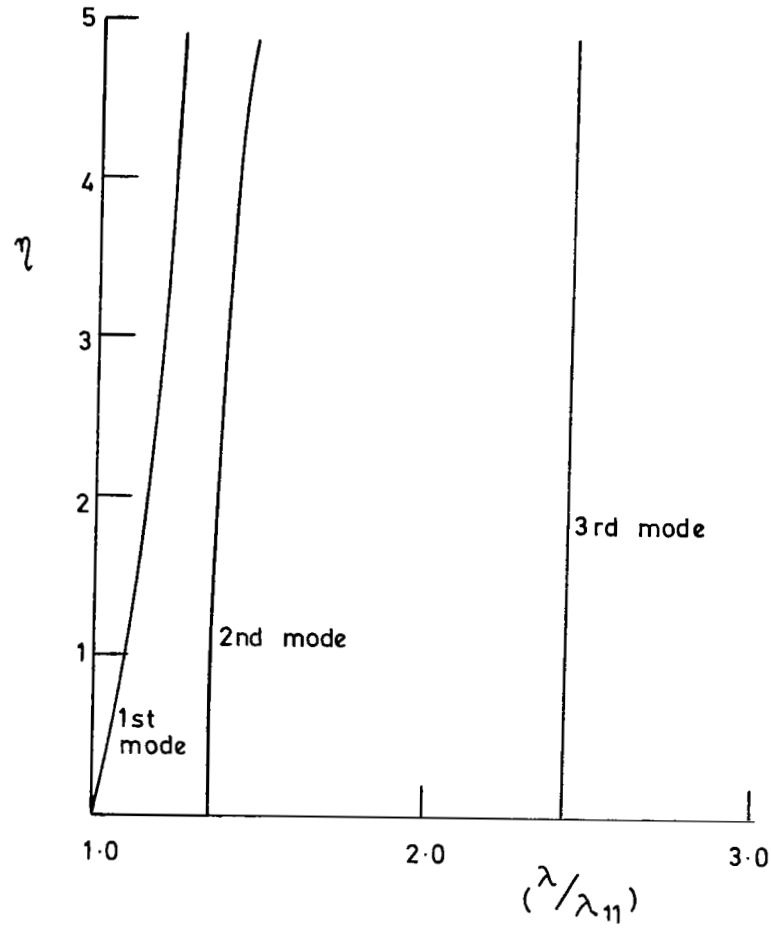

Fig. 5 Variation of natural frequencies ~ η
Clamped case, β = 3·0, 16 element idealisation.

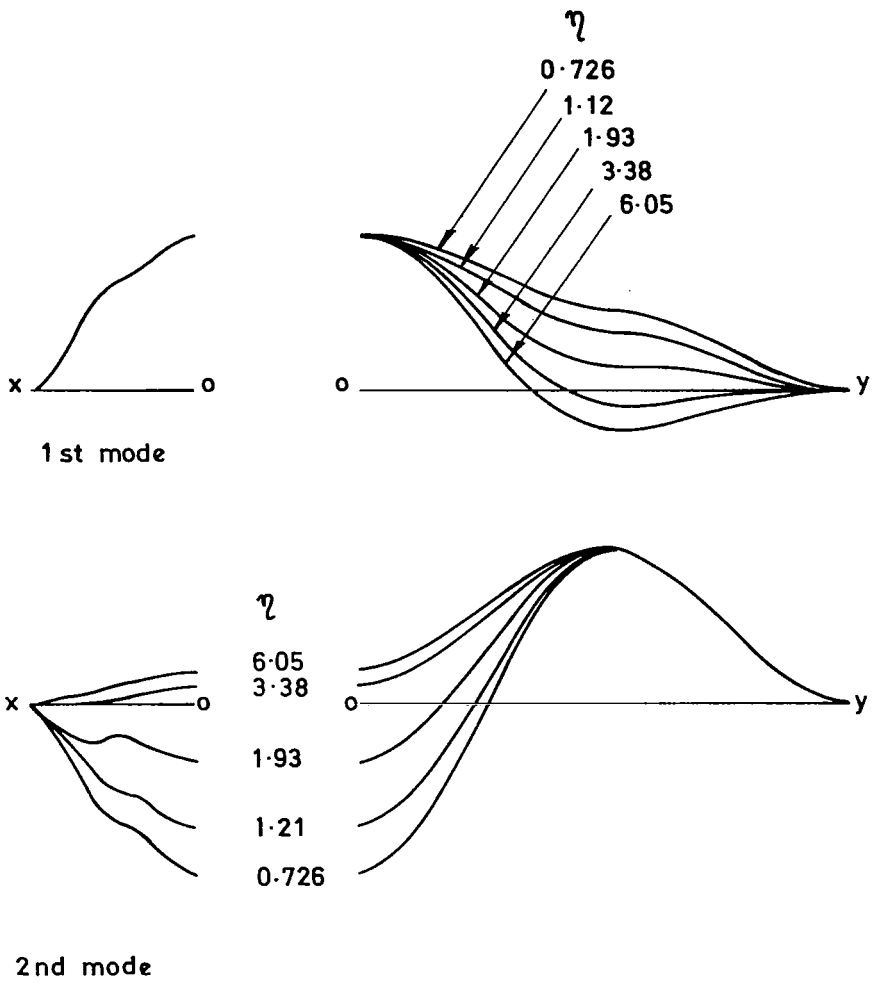

Fig. 6 Variation in mode shapes with η. Simply-supported plate $\beta = 3{\cdot}0$.

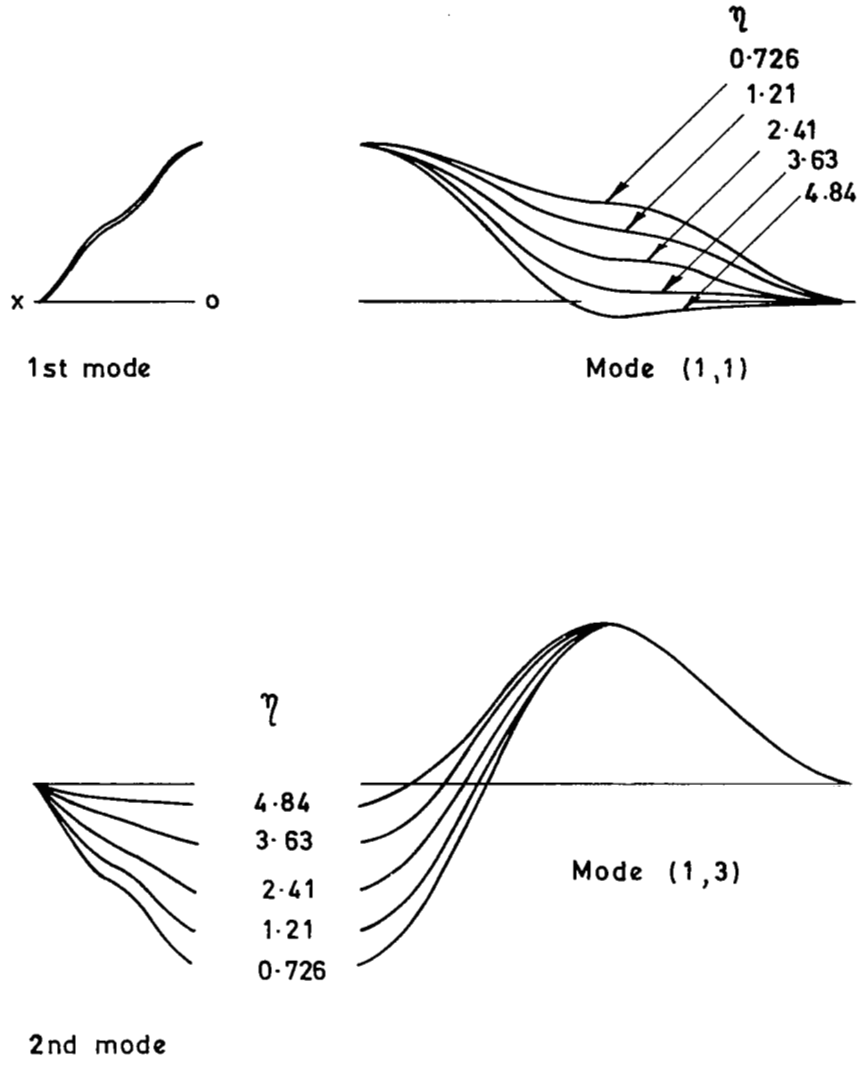

Fig. 7 Variation in mode shape with η. Clamped plate, $\beta = 3 \cdot 0$

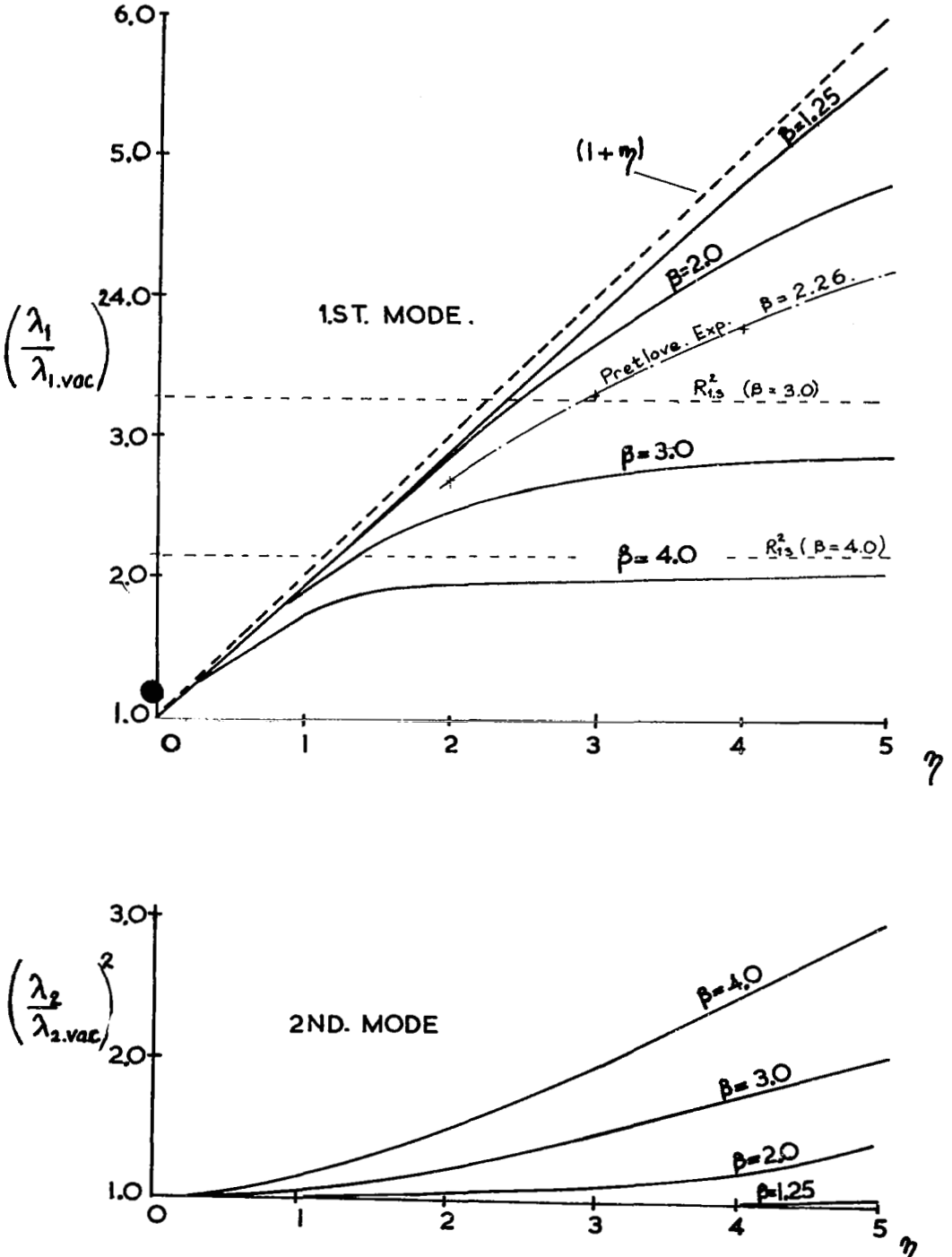

Fig 8 Simply Supported plate: Variation of natural frequencies with η and aspect ratio β

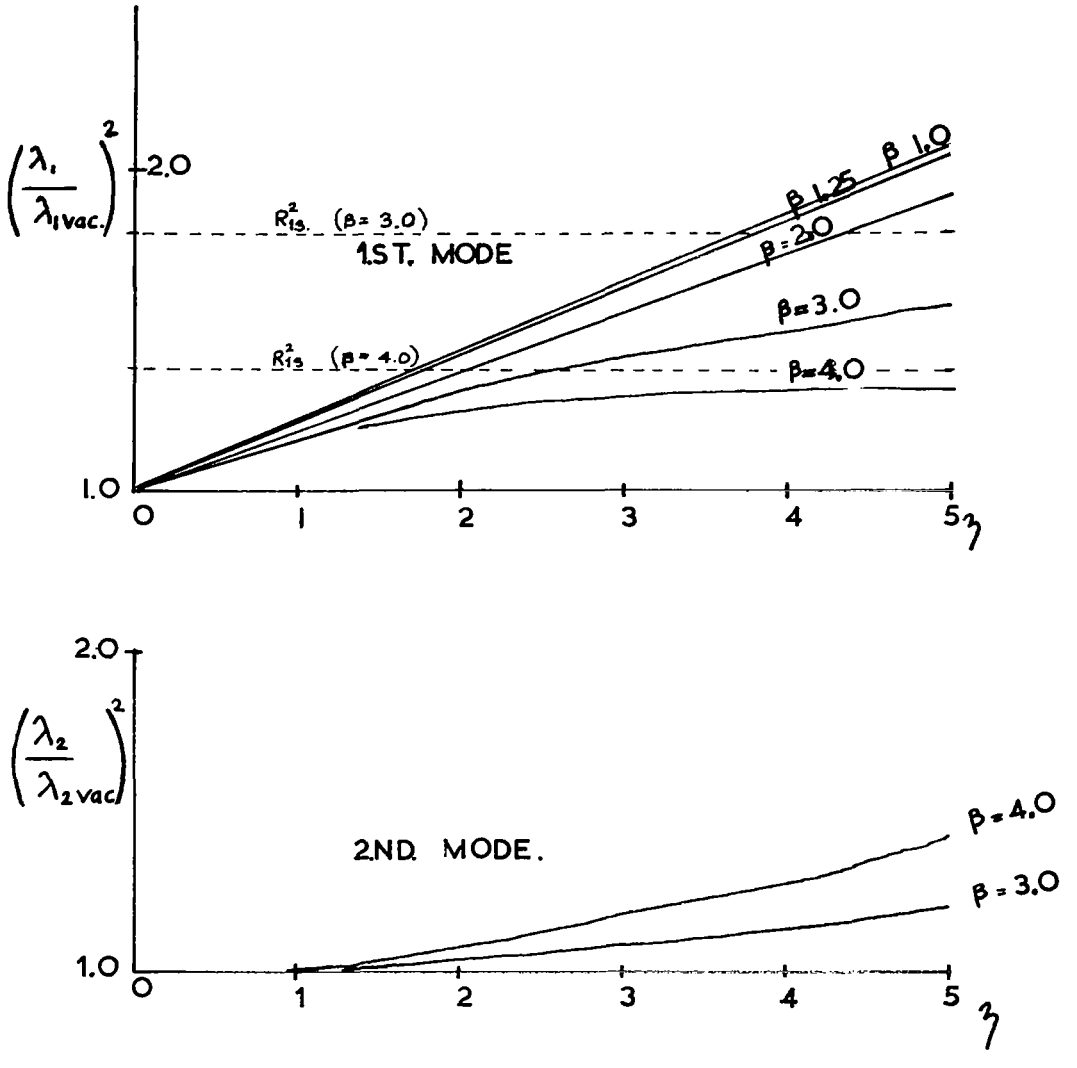

Fig 9 Clamped plate: Variation of natural frequencies with η and aspect ratio β.

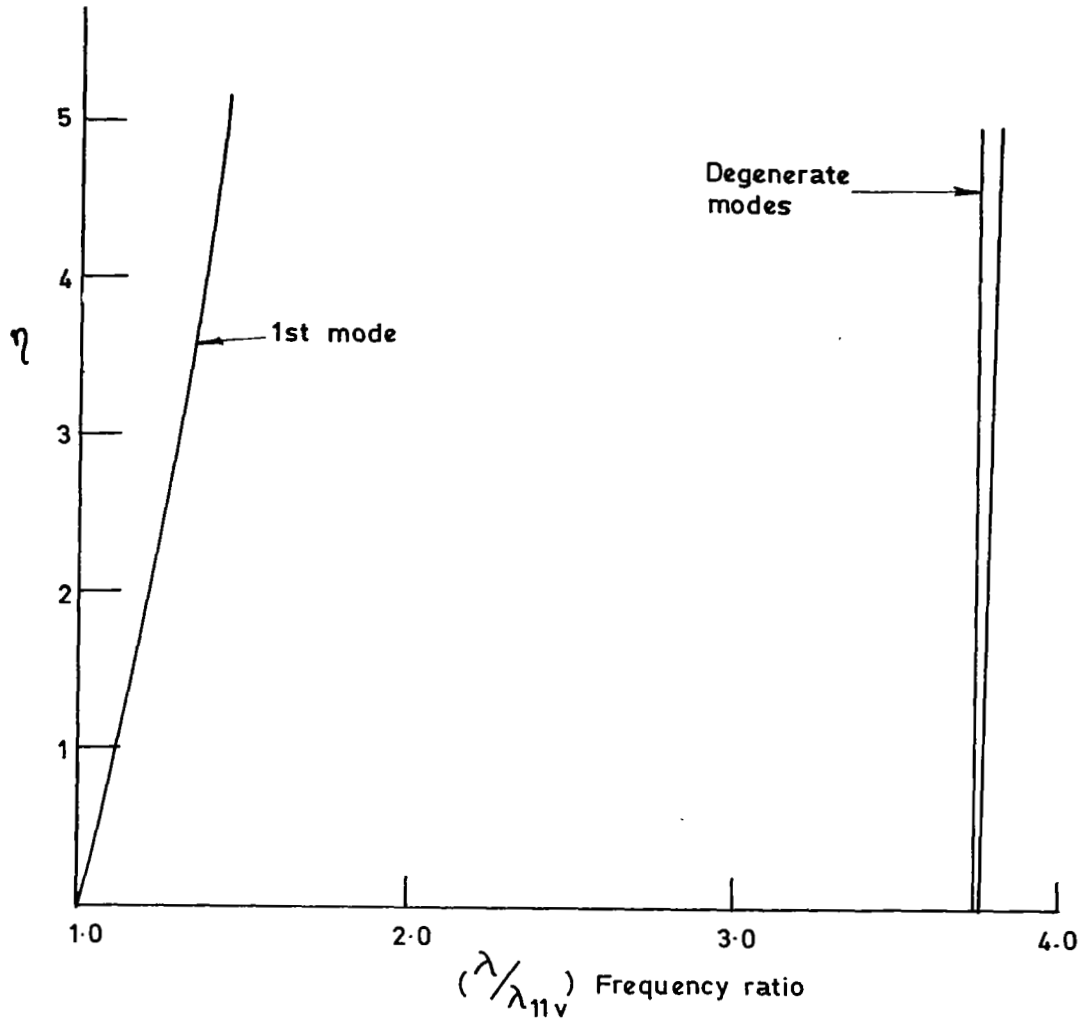

Fig. 10 Square clamped plate; variation of the natural frequencies $\sim \eta$. 16 element idealisation

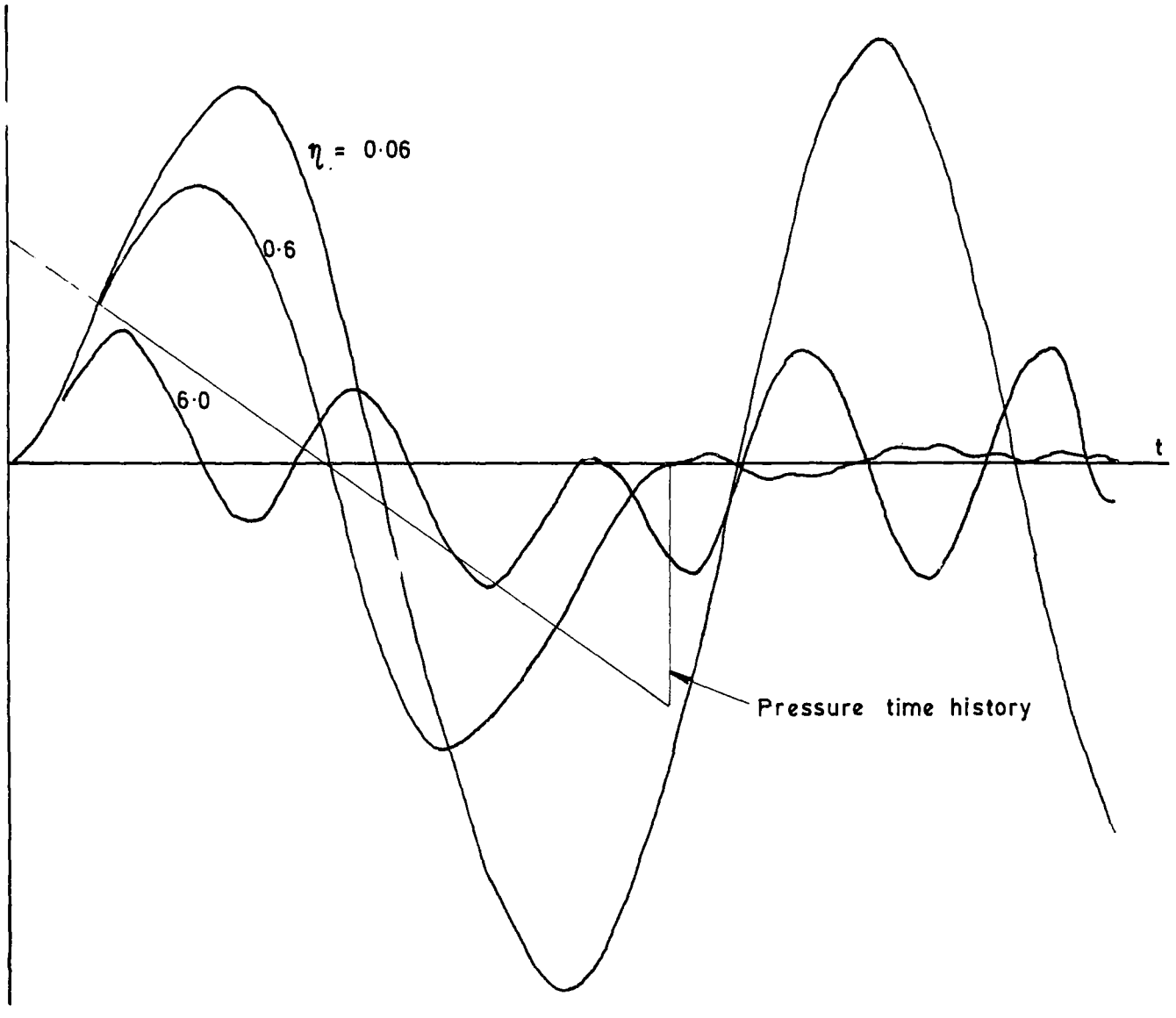

Fig. 11 Displacement response, effect of η. Simply supported plate $\beta = 2{\cdot}0$

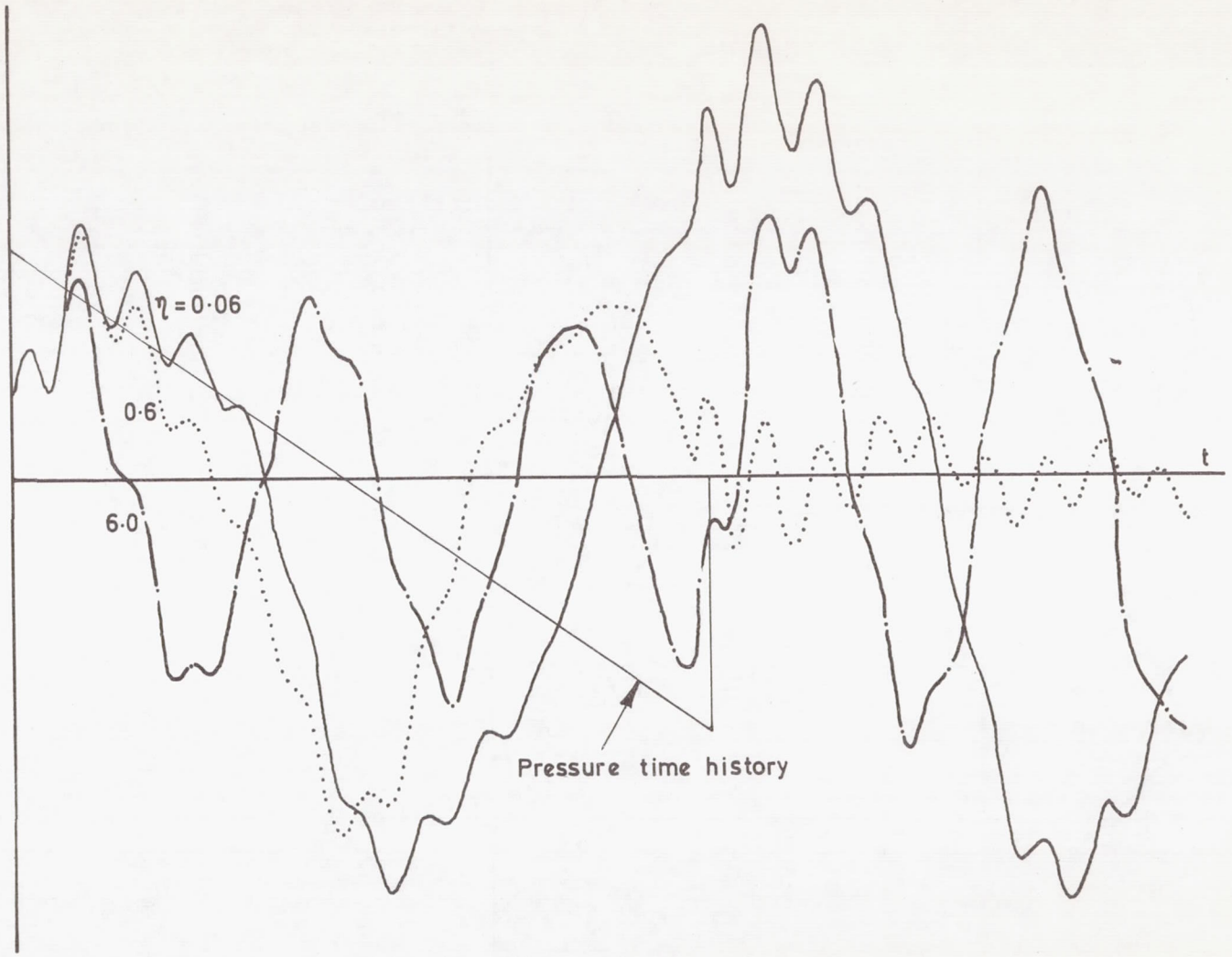

Fig. 12 Velocity response ; effect of η . Simply supported plate $\beta = 2{\cdot}0$

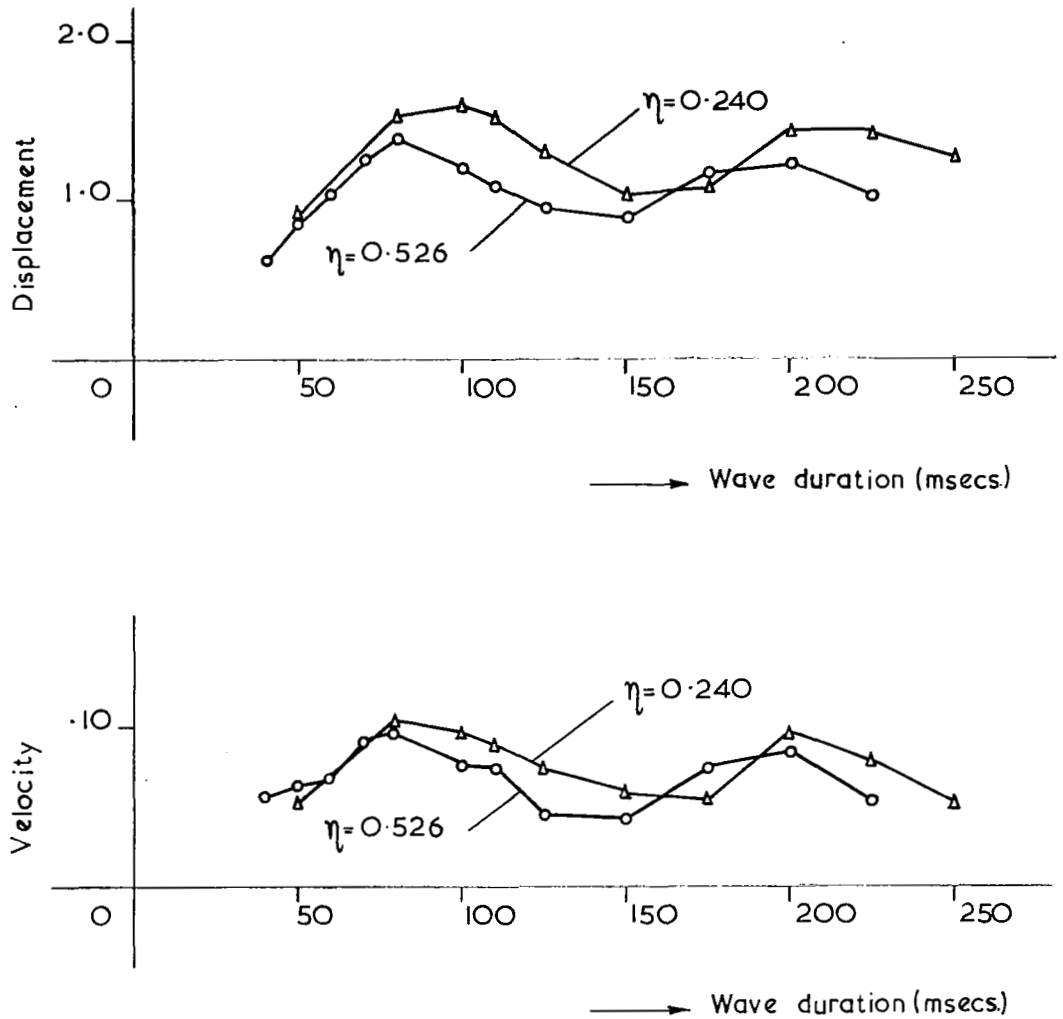

Fig. 13 Displacement and Velocity Shock Spectra for Ideal N wave. Plate Aspect Ratio, $\beta = 2{\cdot}0$ Effect of η.

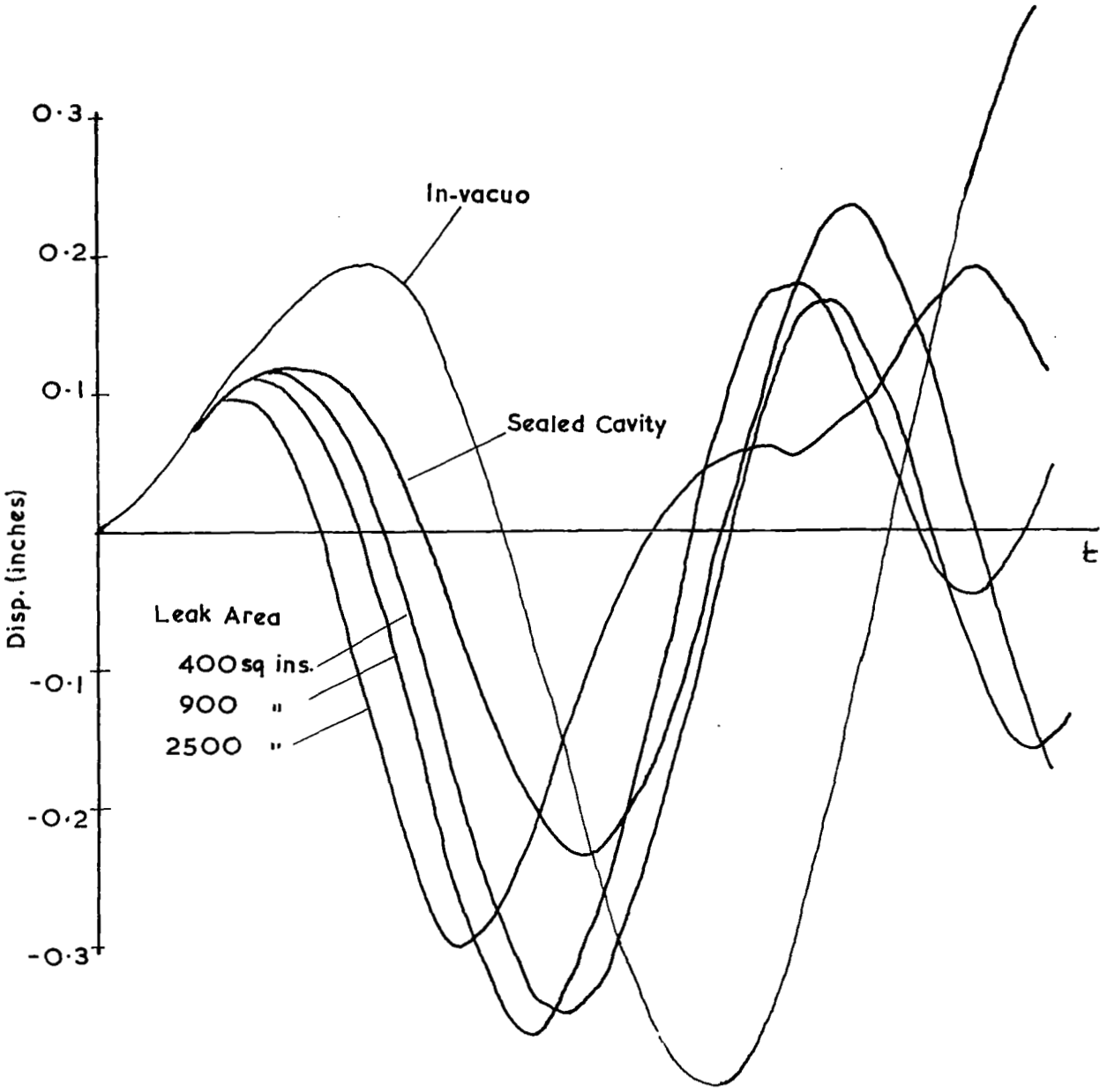

Fig 14 Displacement Response to ideal N wave τ =150ms.
under in-vacuo and various leak openings
Plate dimensions 144x84x0·25
Cavity Volume $3{\cdot}0 \times 10^{6}$ ins.^{3}

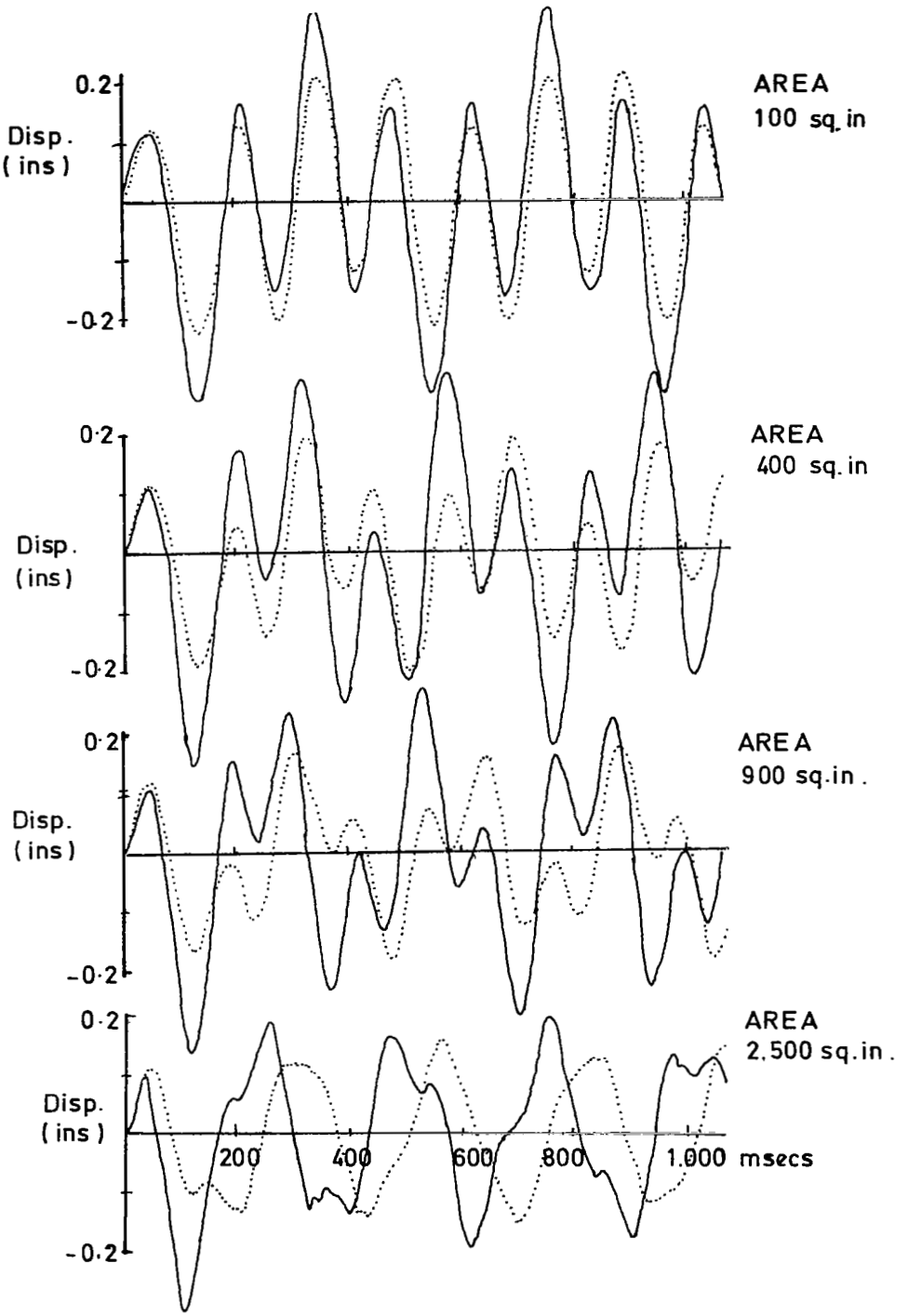

Fig. 15 Displacement responses at plate centre for ideal N wave (τ = 150 ms). Shows effect of opening area and position. —— opening on front face. ..... opening on rear face.

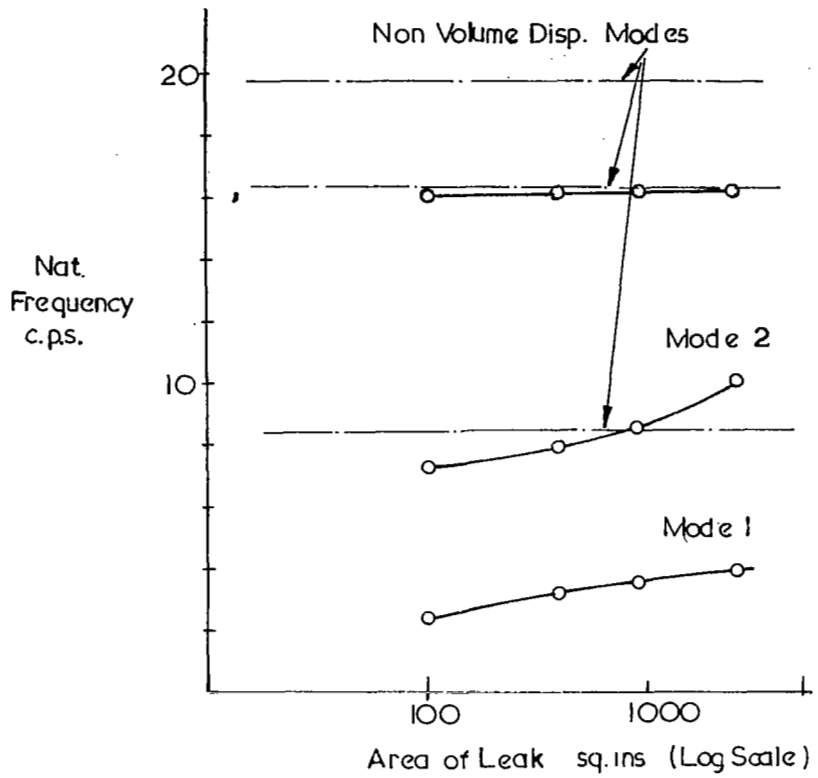

	(Plate Centre Disp)/(Leak Disp.)			
L. Area sq. ins.	100	400	900	2500
Mode 1	-.012	-.054	-.131	-.405
Mode 2	.058	.108	.150	.250

Fig 16 Details of Nat. Frequencies with various Leak Areas
Plate Dimensions 144 X 84 X 0.25
Cavity Volume 3.0×10^6

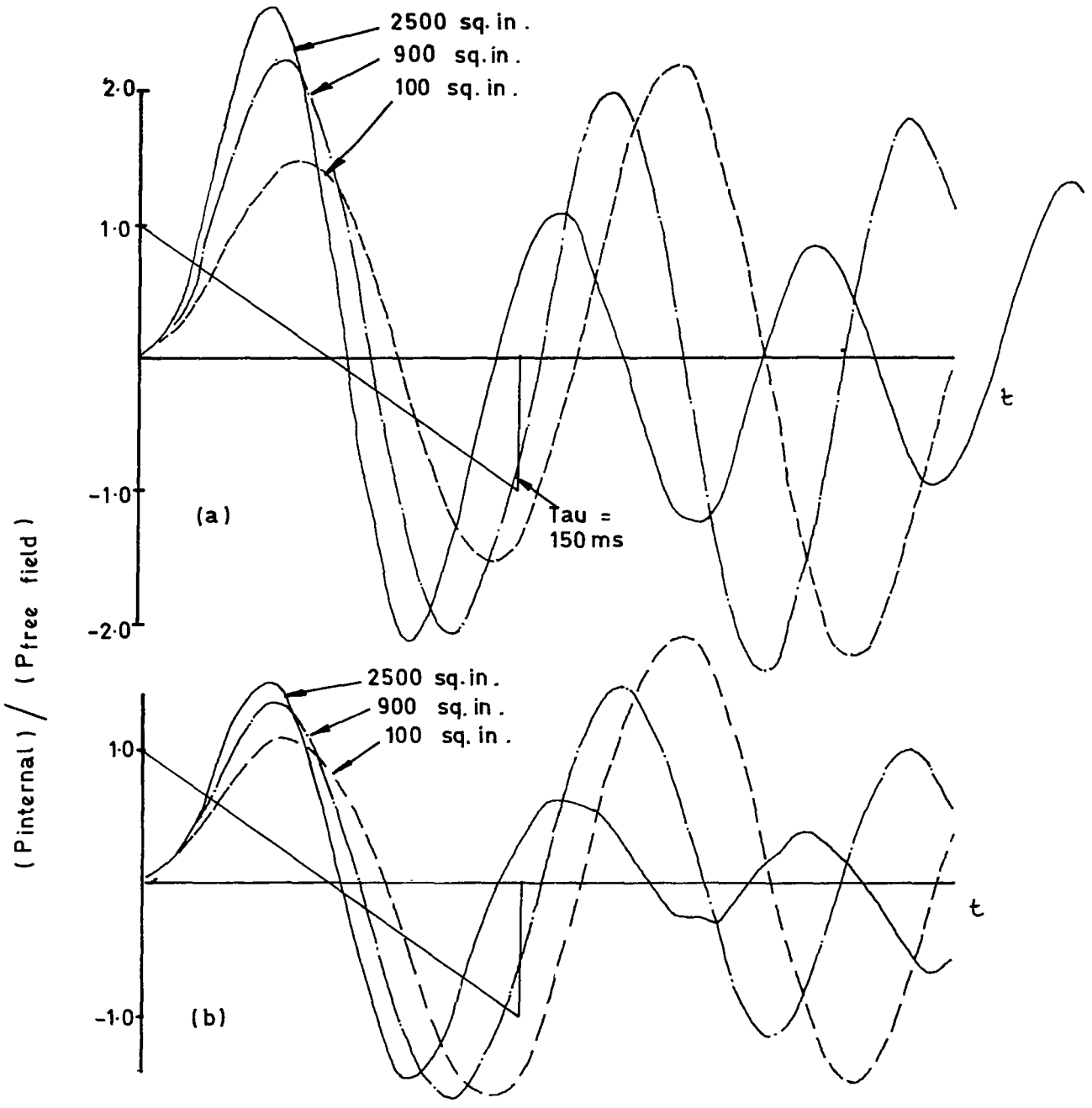

Fig. 17 Internal cavity pressure ratios for various opening areas. N wave at normal incidence on the front face : (a) opening on front face. (b) opening on back face.

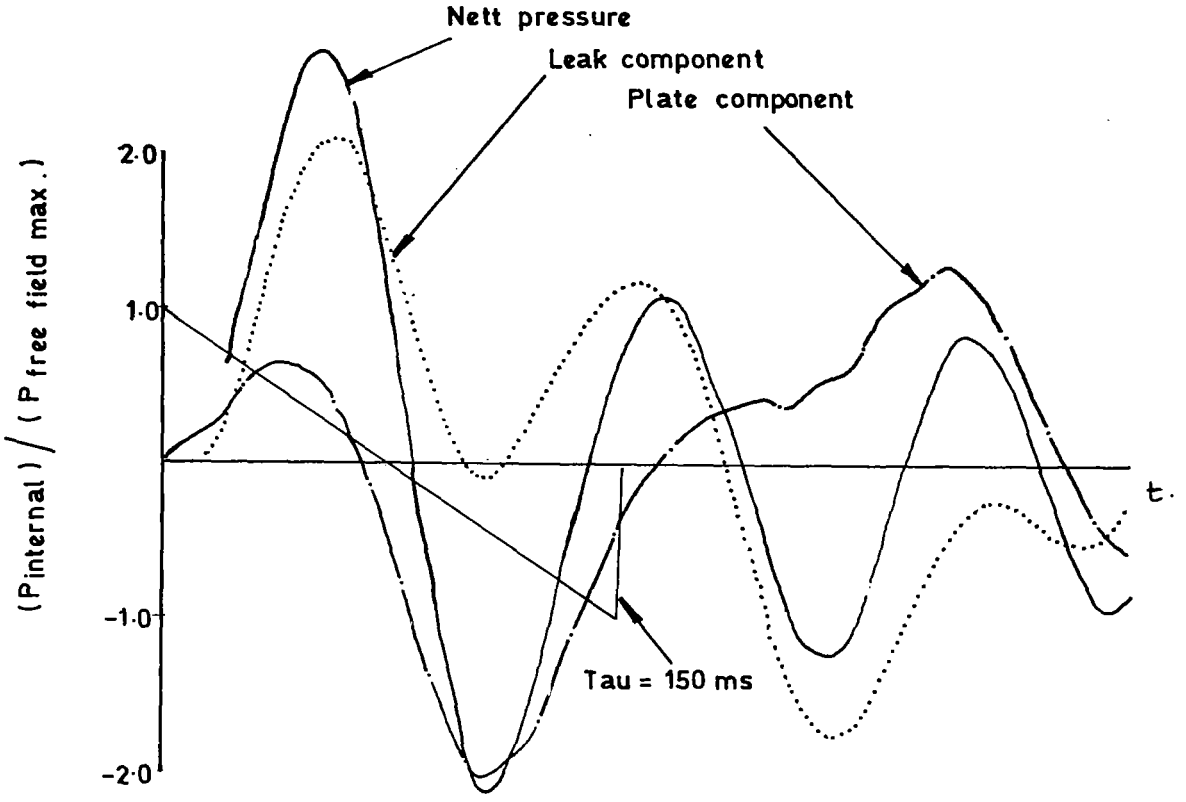

Fig.17 (c) Internal cavity pressure ratio for 2500 sq.in. opening showing contributions from the plate and leak components. Plate and leak on the front face.

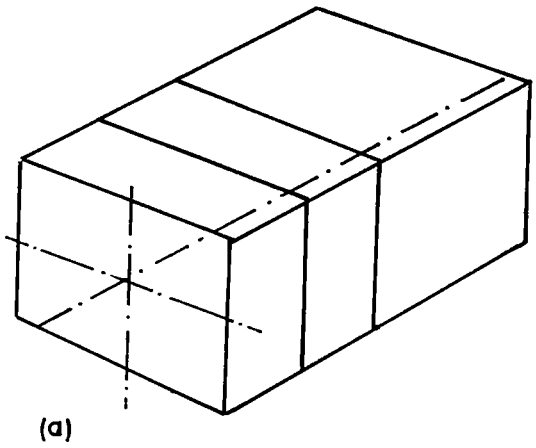

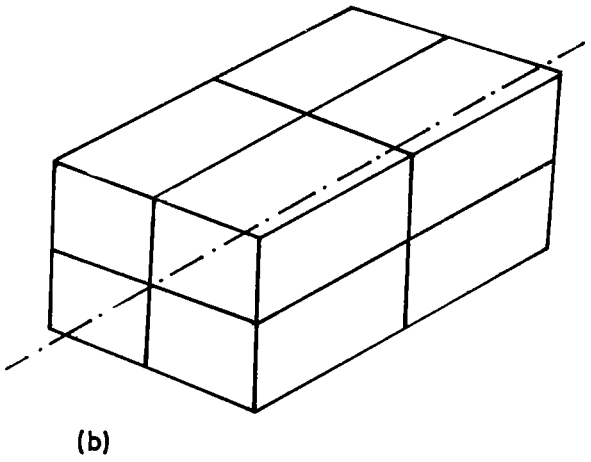

Fig. 18 Models for acoustic element eigenvalue problem

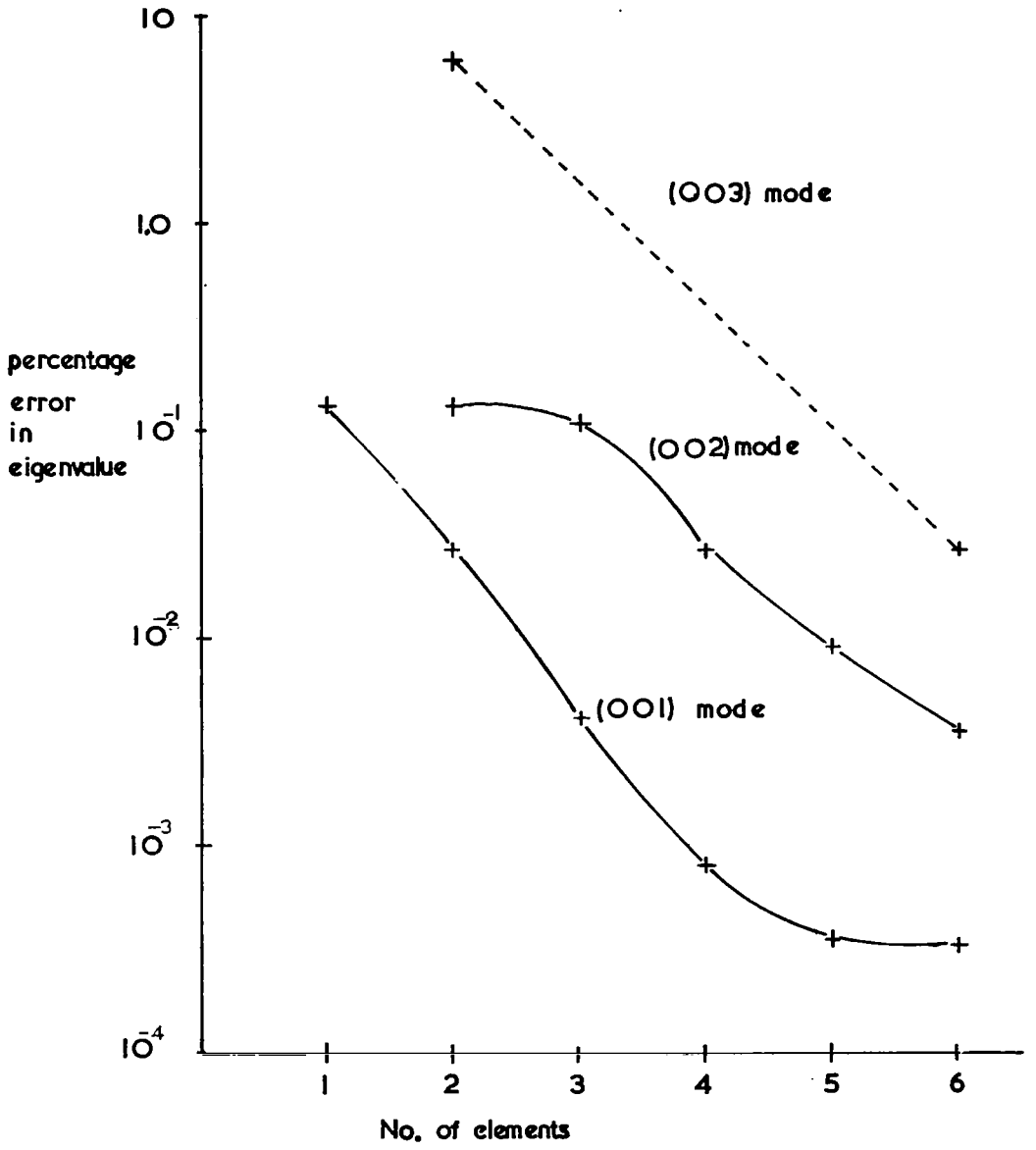

Fig 19 Convergence of eigenvalues with number of acoustic elements for a hard walled box cavity

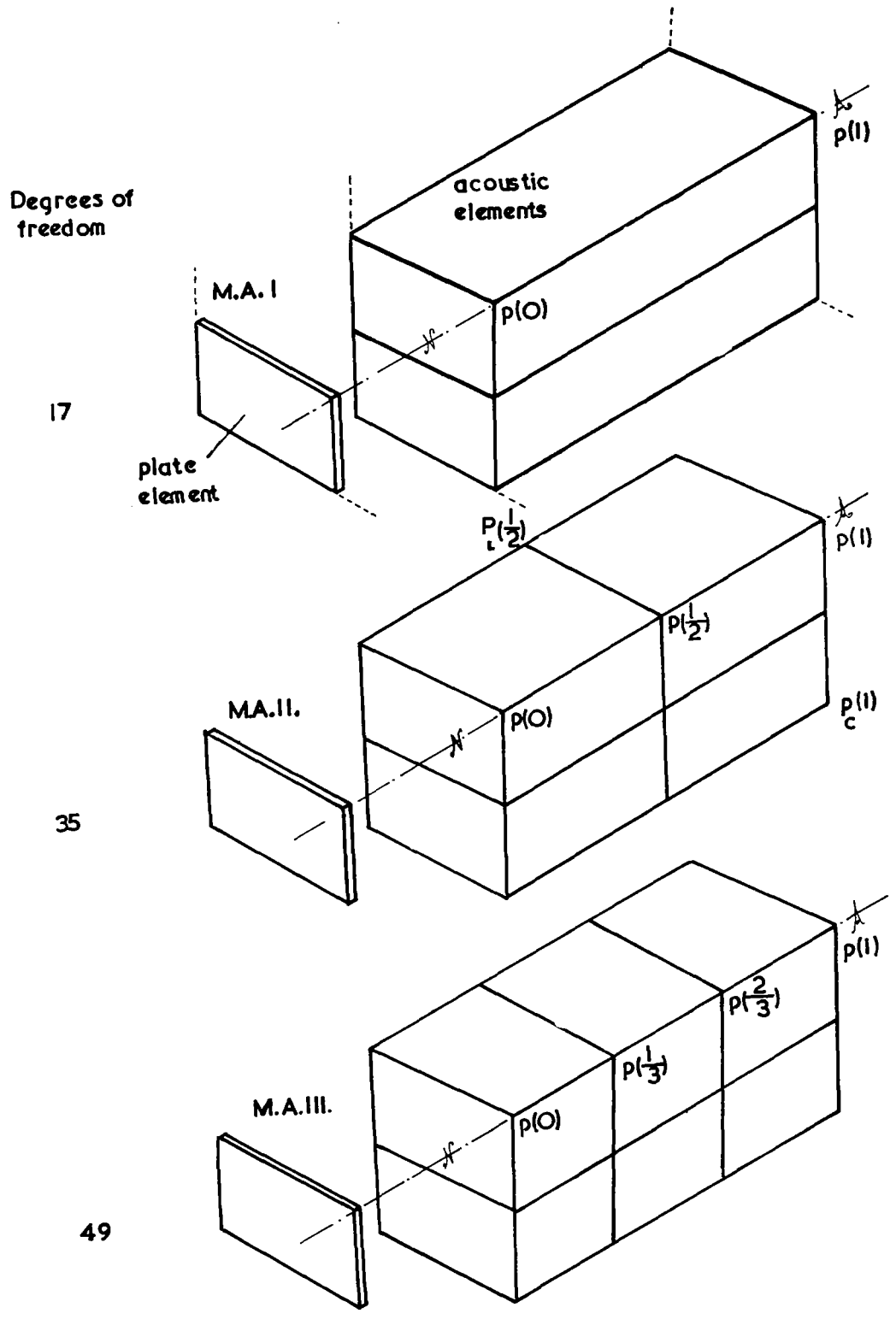

Fig 20 The finite element models of plate room system

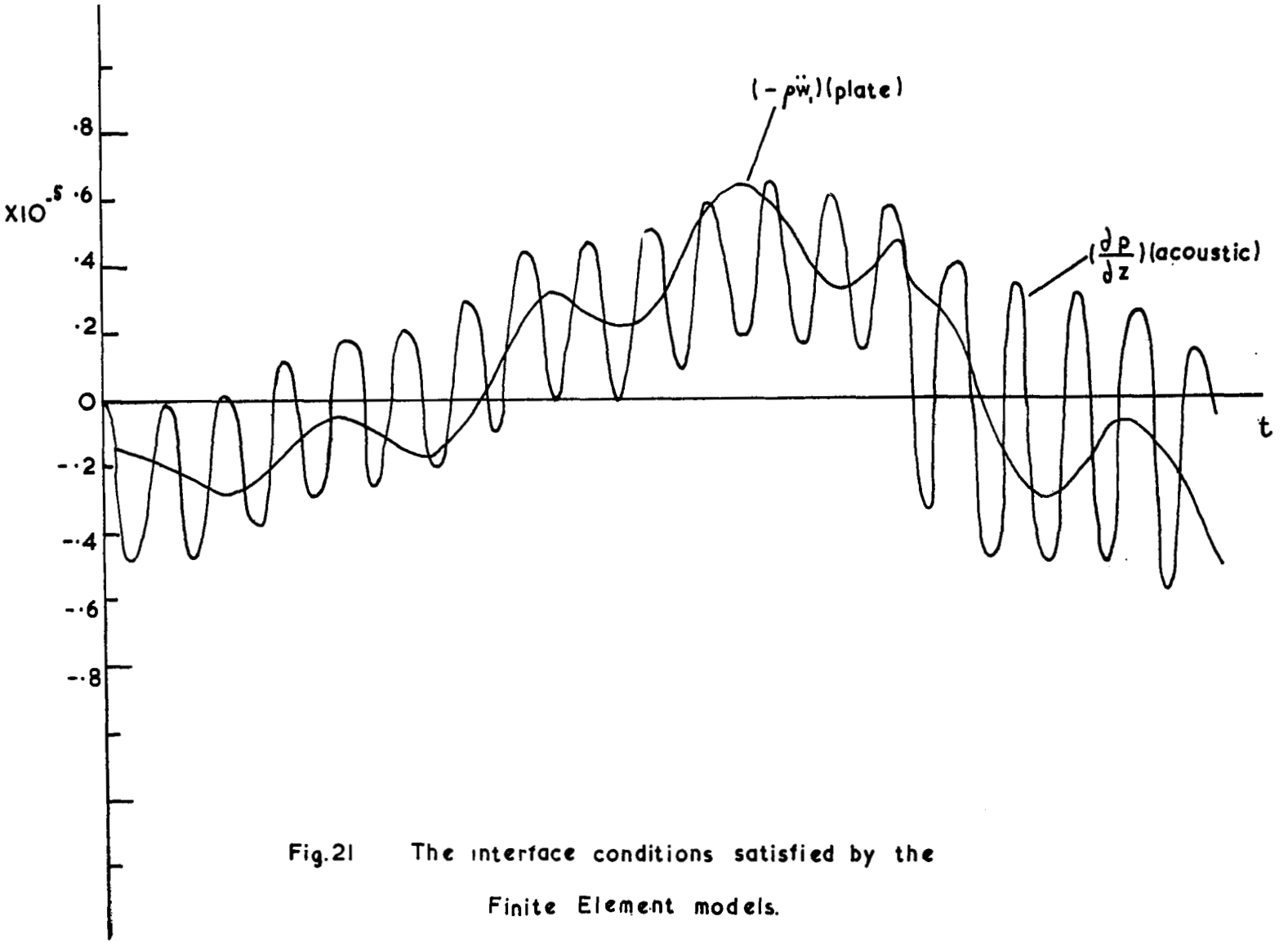

Fig.21 The interface conditions satisfied by the Finite Element models.

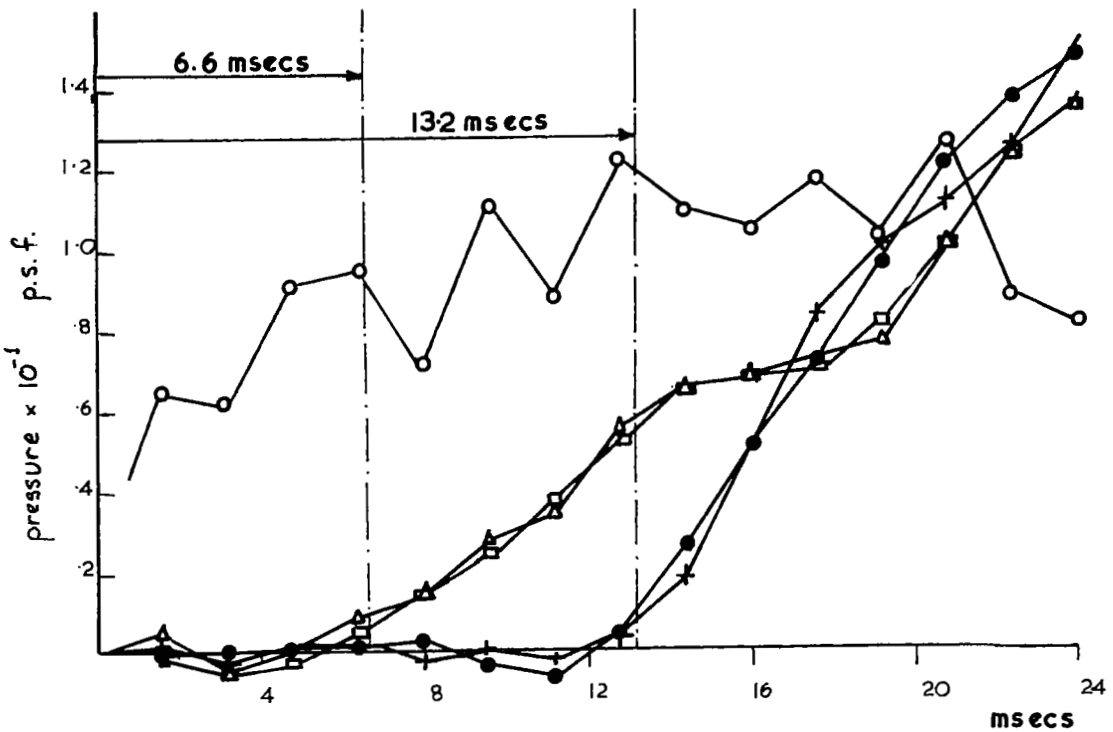

o	$p(0)$
Δ	$p(\frac{1}{2})$
+	$p(1)$
□	$p_L(\frac{1}{2})$
●	$p_c(1)$

Fig. 22 Comparison between exact and approximate delays for pressure response in room

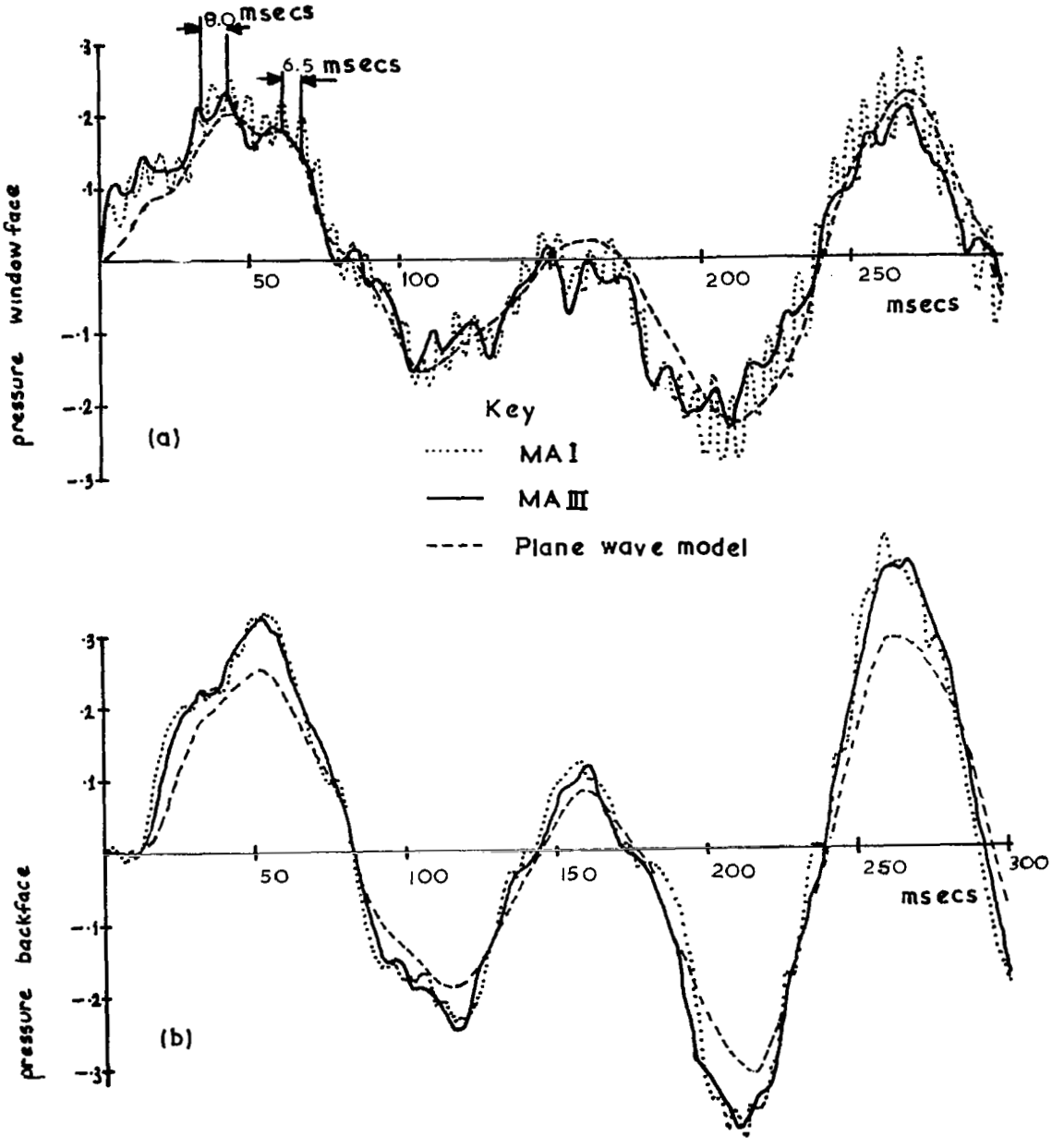

Fig. 23 Comparison of MA I, MA III, and Plane wave model results

(a) Pressure at front face (b) Pressure at back face

τ = 200 msecs.

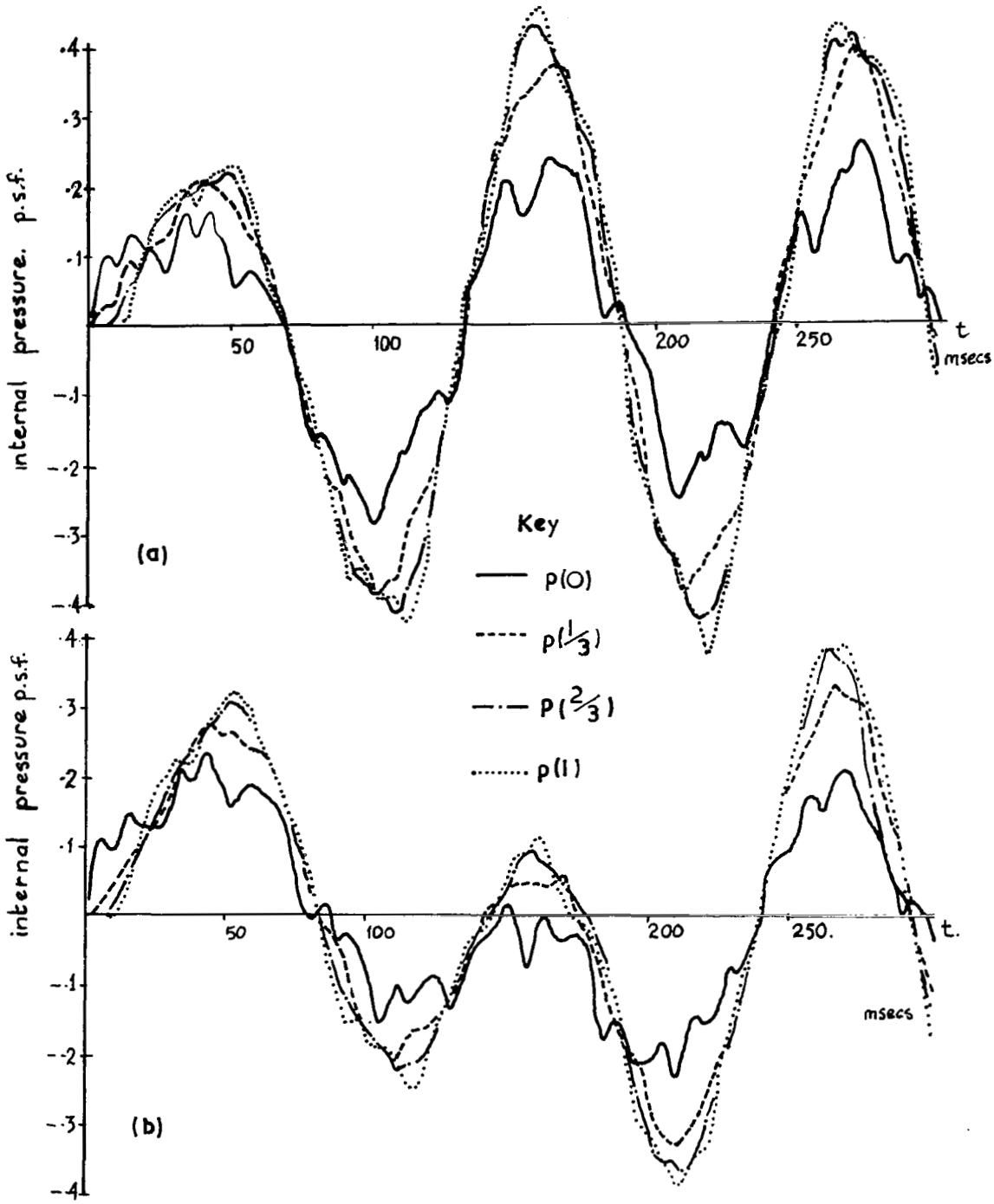

Fig. 24 Pressure at Intermediate Positions using MA III

(a) τ = 100 msecs (b) τ = 200 msecs . Max . inc. pressure 1.0 p.s.f.

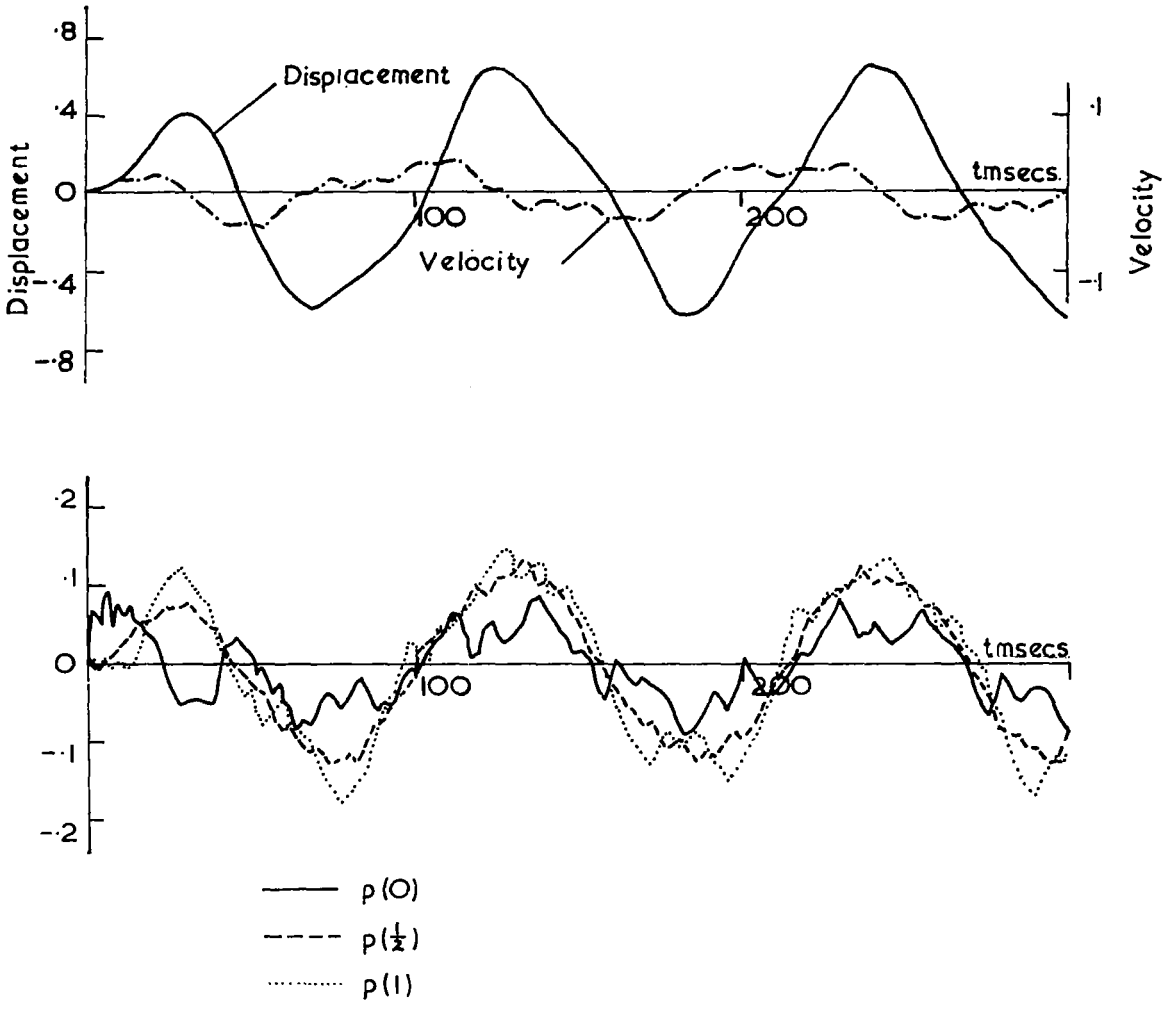

Fig. 24 (a) Displacement and Velocity responses at Plate Centre Pressure Responses. TAU = 40 msecs

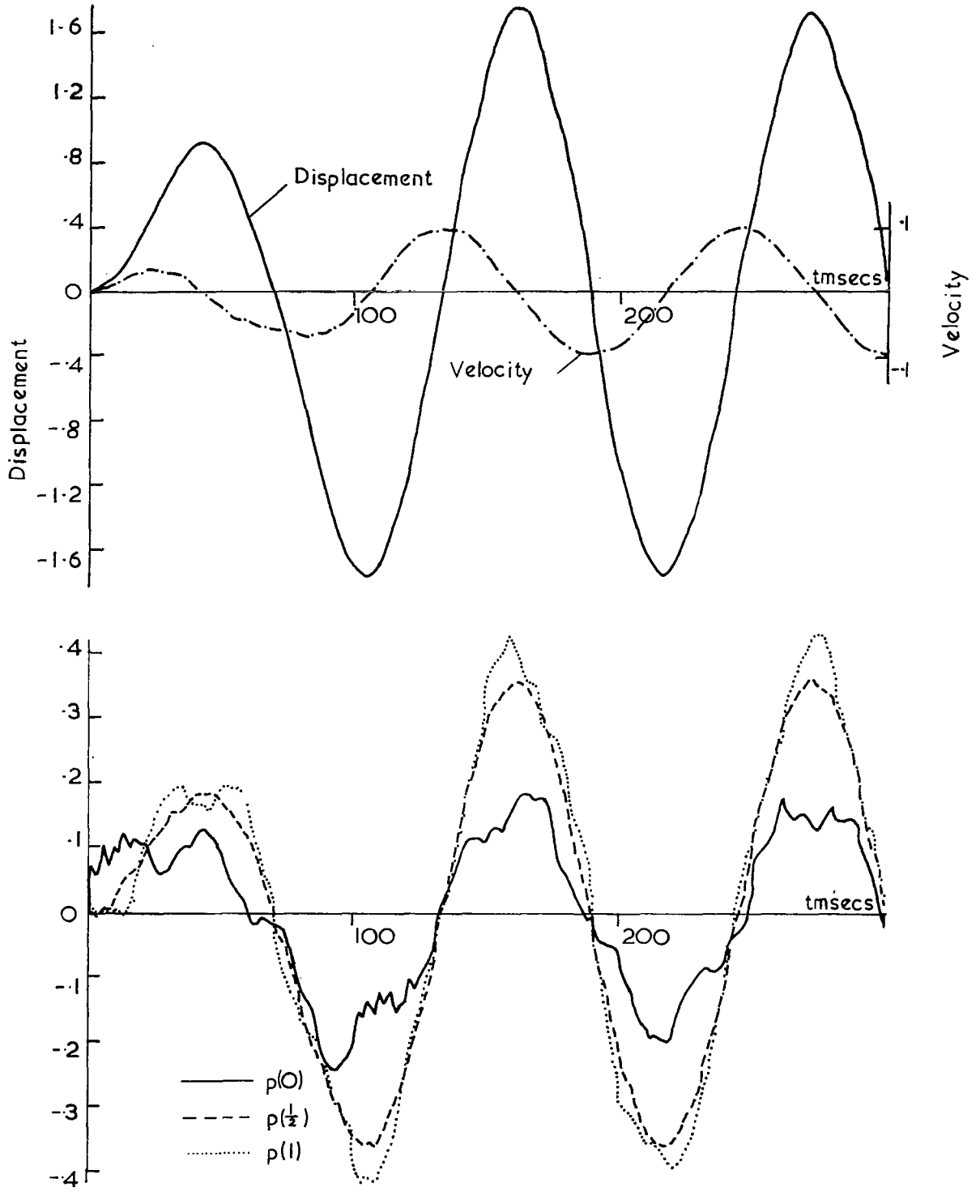

Fig 24(b) Displacement and Velocity responses at Plate Centre

Pressure Responses TAU = 100 msecs.

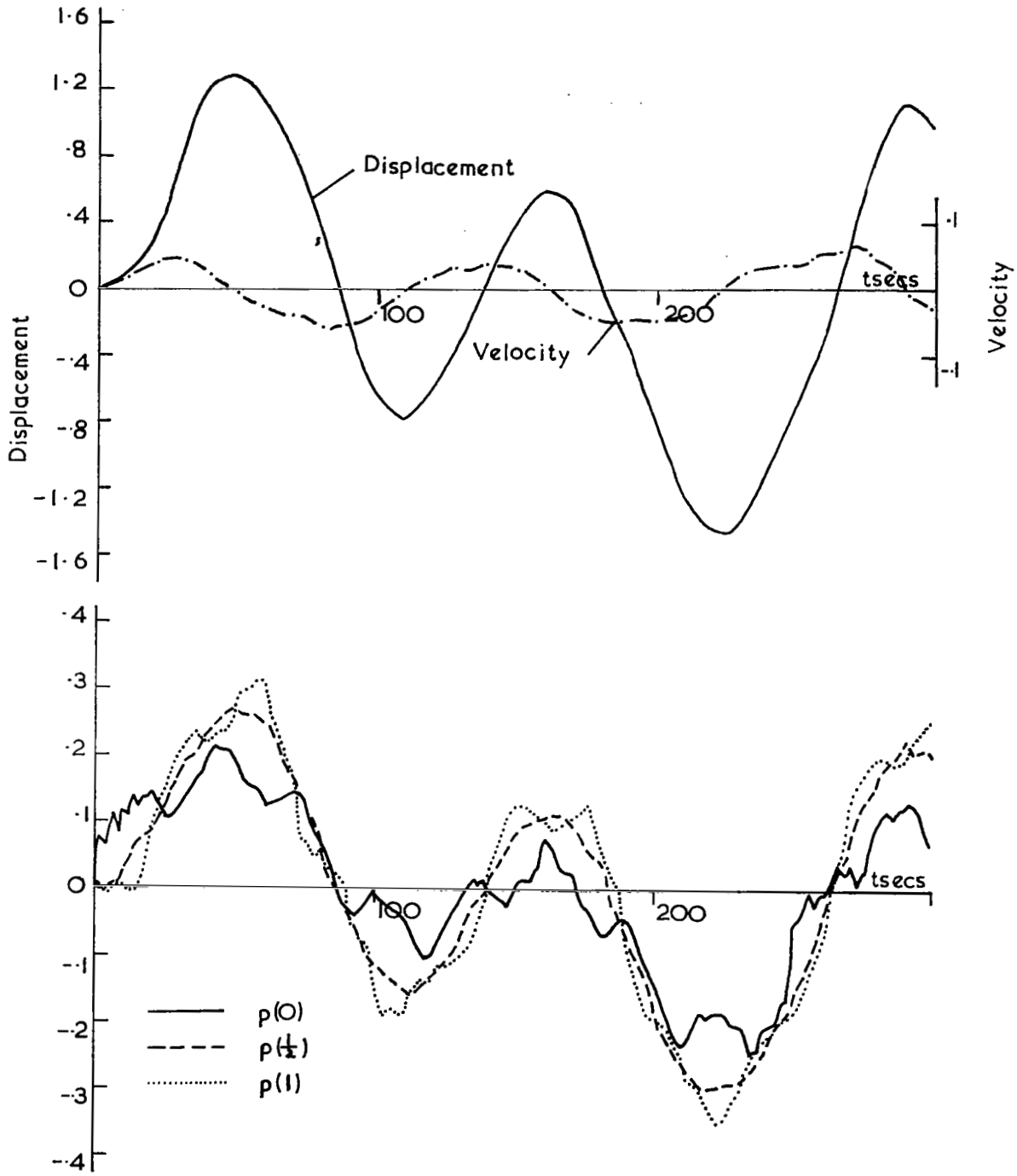

Fig. 24(c) Displacement and Velocity responses at Plate Centre
Pressure Responses. TAU = 250 msecs.

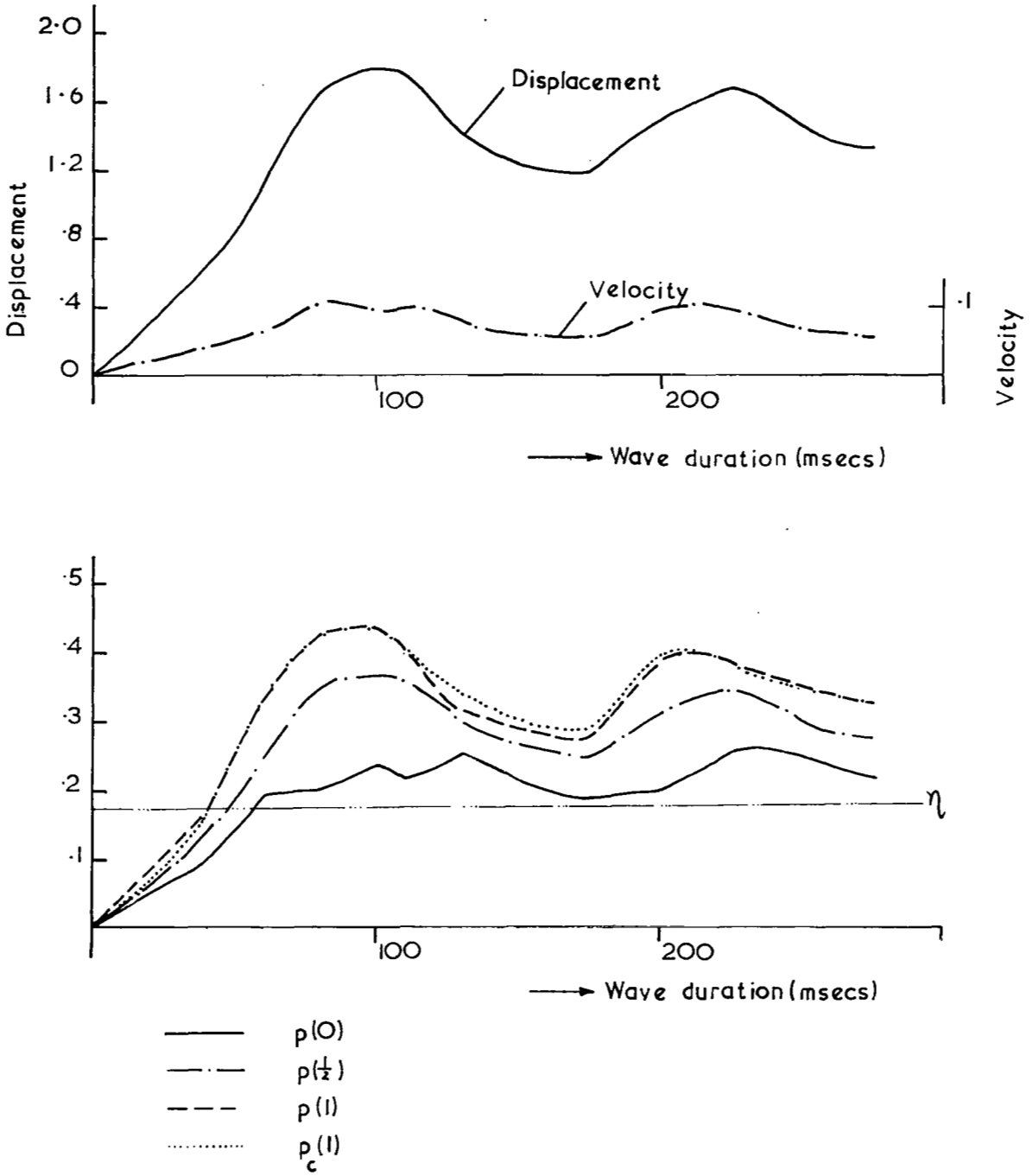

Fig. 25 Shock Spectra : Ideal N wave : Maximum Plate and Acoustic Responses.

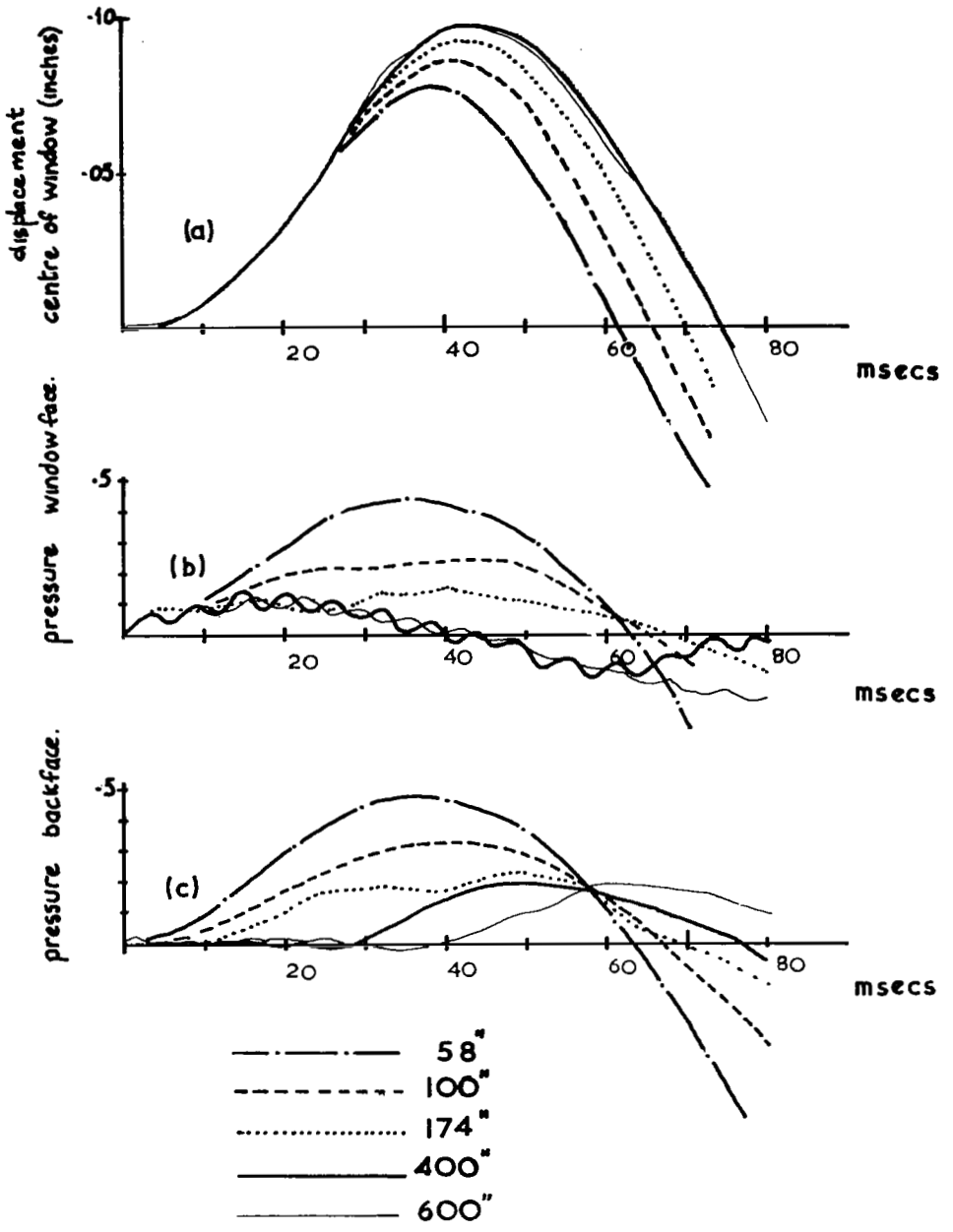

Fig 26 . Effect of cavity depth.

window 120" x 60" x 0.25"

cavity 120" x 120" x depth.

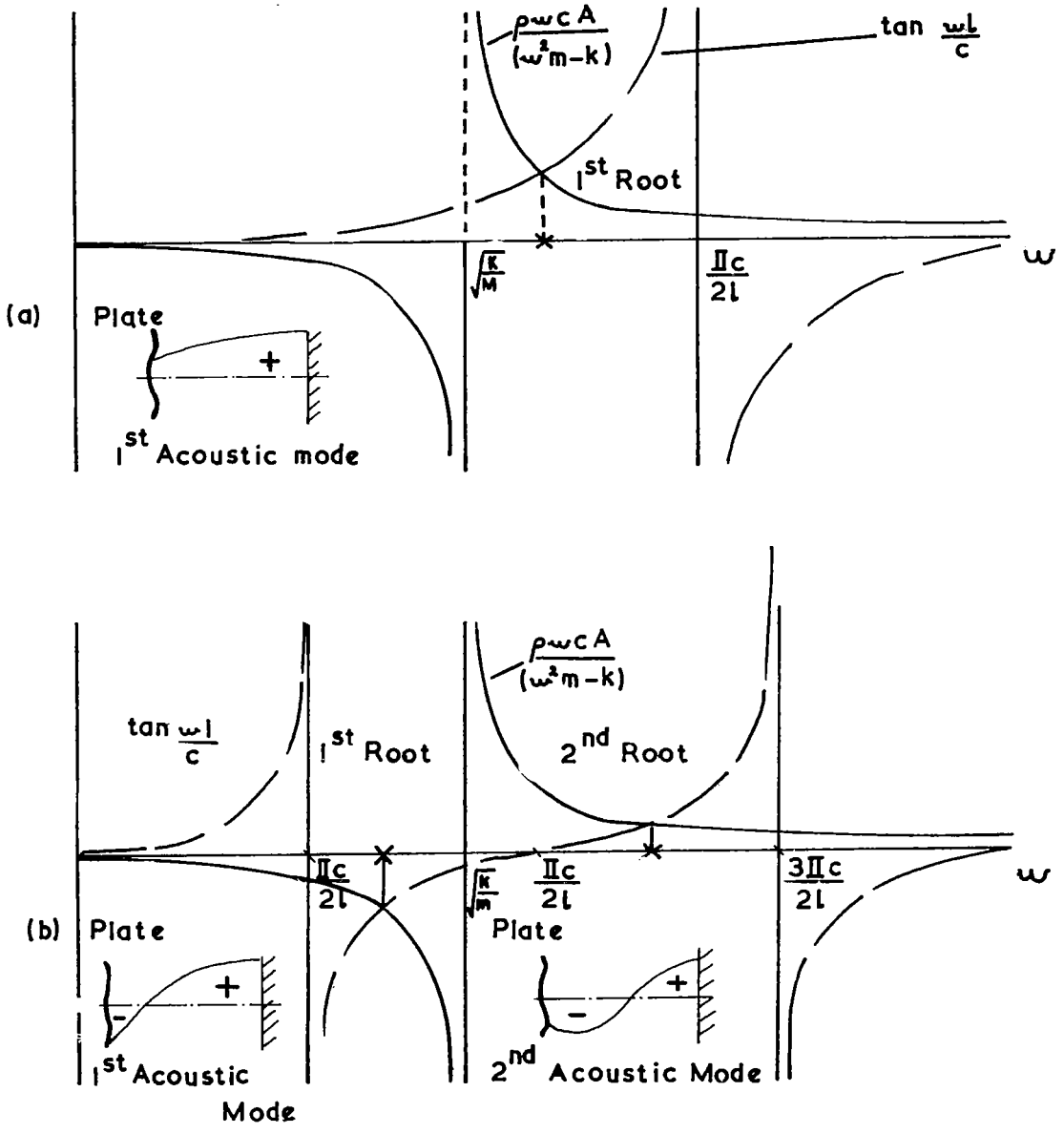

Fig. 27 Graphical Solution for Roots of Coupled oscillator

(a) Small depth (b) Large depth

NASA-Langley, 1969 — 23 CR-1421